

LB/TH/44/2025

TH6030

**MAXIMUM PERMISSIBLE SLOPE FOR
INTERLOCKING CONCRETE BLOCK PAVING FOR
RESIDENTIAL ROADS**

C.J. Atapattu

219565T

Master of Engineering in Highway and Traffic Engineering

Department of Civil Engineering

Faculty of Engineering

University of Moratuwa

Sri Lanka

July 2025

**MAXIMUM PERMISSIBLE SLOPE FOR
INTERLOCKING CONCRETE BLOCK PAVING FOR
RESIDENTIAL ROADS**

C.J. Atapattu

219565T

Dissertation submitted in partial fulfillment of the requirements for the degree
Master of Engineering in Highway and Traffic Engineering

Department of Civil Engineering
Faculty of Engineering

University of Moratuwa
Sri Lanka

July 2025

DECLARATION

I affirm that this dissertation is my original work and does not incorporate, without proper acknowledgment, any material previously submitted for a degree or diploma at any other university or institution. To the best of my knowledge, it does not contain any material previously published or written by another person, except where such references are clearly cited in the text.

Furthermore, I authorize the University of Moratuwa to reproduce and distribute this thesis/dissertation, in whole or in part, in both print and electronic formats. I retain the right to use all or part of this material in future publications, such as journal articles or books.

Signature:

Date: 24/07/2025

I hereby certify that the candidate has carried out the research presented in this Master's thesis/dissertation under my supervision. I confirm that, to the best of my knowledge, the declaration made by the candidate above is accurate and correct.

Name of Supervisor: Prof. W. K. Mamperachchi

Signature of the Supervisor:

Date: 28/07/2025

ABSTRACT

Concrete Block Paving (CBP) is a popular surfacing method currently used for rural roads in Sri Lanka, primarily due to its cost-effectiveness, ease of construction, and suitability for medium- to low-traffic conditions. Nowadays, CBP is applied not only on flat terrains but also on steep slopes. Determining the maximum permissible slope for block paving is critical to ensuring the durability, stability, and functionality of the pavement system. Empirical studies and field observations show that gradients exceeding permissible limits can lead to problems such as erosion, block displacement, and reduced skid resistance, especially over unsealed subgrades.

While several studies have examined the influence of block shape, laying pattern, laying angle, joint width, and block thickness on CBP performance in flat terrain, these factors may behave differently on sloped surfaces due to additional forces acting on the blocks. Therefore, the aim of this research is to investigate the maximum permissible slope for CBP under medium- to low-traffic conditions.

As part of the study, a 90-meter road segment with slopes ranging from 0° to 10° was constructed. Paving was done at 10-meter intervals using Uni-style blocks, while varying the block patterns, laying angles, and cross beam intervals. Field data were used to calculate relative vertical deflections. A Finite Element Model (FEM) was also developed in ANSYS software to simulate the behavior of the pavement system by varying slope, laying pattern, laying angle, and cross beam spacing.

The results indicate that as slope increases, horizontal deflection tends to increase while vertical deflection decreases. However, when cross beams are placed at optimal intervals, both horizontal and vertical deflections become negligible. Under such conditions, the effects of slope, laying pattern, and laying angle on pavement performance are significantly reduced, making CBP a viable option for rural roads even on sloped terrains.

Keywords: Concrete Block Paving (CBP), Finite-element model (FEM), uni style block pattern, Herring bond pattern.

ACKNOWLEDGEMENT

I would like to gratefully acknowledge the valuable guidance and support of everyone who contributed to the success of this M.Eng. research project. I sincerely appreciate their assistance and take this opportunity to extend my heartfelt thanks.

First and foremost, I express my deepest gratitude to my research supervisor, Prof. W.K. Mampearachchi, for his invaluable guidance, unwavering support, and continuous encouragement throughout the course of this study. His direction, from the beginning to the successful completion of the project, was truly instrumental.

I also extend my sincere appreciation to Mr. R.P. Tharanga, Executive Engineer, and his team at the Road Development Authority, Matara, for their generous support in facilitating the trial section and assisting with data collection—an essential component of this research.

My thanks also go to the Department of Civil Engineering, University of Moratuwa, for providing me with the opportunity and the necessary resources to undertake this study.

I take this opportunity as well to thank all the lecturers who imparted their knowledge throughout my Master of Engineering degree and those who offered valuable insights that helped shape this project.

Lastly, I express my heartfelt thanks to my family, whose constant support, encouragement, and timely assistance provided the foundation that allowed me to focus and complete this work successfully.

TABLE OF CONTENTS

1. Introduction.....	1
1.1. Background.....	1
1.2. Problem Statement	2
2. Objectives	4
3. Literature Review	5
3.1. Effect of laying pattern.....	5
3.2. Effect of Block shape	7
3.3. Effect of laying angle	8
3.4. Effect of joint width	9
3.5. Effect of paver thickness	9
3.6. Effect of degree of the slope	10
3.7. Effect of cross beams	10
4. Methodology.....	11
4.1. Monitoring of existing block paved roads in sloped sections.....	11
4.2. Developing trail concrete block surface	14
4.3. Analysis of Field data.....	15
4.4. Finite Element modelling of CBP	16
4.5. ANSYS Workbench for finite Element model analysis	17
4.6. Validation of the ANSYS Finite Element model.....	20
5. Results and Analysis	23
5.1. Outcomes of developed trail Concrete block surface.....	23
5.2. Outcomes of FEM Model.....	26
5.3. Optimum spacing of cross beams	33
6. Conclusion	40
7. Limitations and Recommendations.....	42
8. References	44
9. Appendix	45

LIST OF FIGURES

Figure 1: Deformation and horizontal creep of CBP for sloping road section (Mudiyono, 2015).....	2
Figure 2: Loading positions vs vertical deflection(different laying patterns).....	5
Figure 3: Loading position vs H. deflection (Different laying patterns)	6
Figure 4: Horizontal force vs Horizontal creep to analyze the effect of laying pattern.....	6
Figure 5: Effect of block shapes on deflection.....	7
Figure 6: Loading point vs deflection (deflection profile).....	7
Figure 7: The effect of laying angle.....	8
Figure 8: Horizontal force vs Horizontal creep(effect of width of joints)	9
Figure 9: Horizontal force vs Horizontal creep (The effect of thickness of paving)...	9
Figure 10: The effect degree of slope	10
Figure 11: Sloping of anchor beams	10
Figure 12: 12° sloped block paved road.....	11
Figure 13: Common field practice of placing cross spacing	13
Figure 14: Standard method of placing cross beams	13
Figure 15: Block placing in trail section	14
Figure 16: Finished trial block paved road section.....	15
Figure 17: Identification of wheel path in completed trail road section	15
Figure 18: Surface level checking using Automatic level instrument	16
Figure 19: Mesh developed in ANSYS Workbench.....	17
Figure 20: Geometry developed with ANSYS Workbench.....	18
Figure 21: Load application as horizontal and vertical components	19
Figure 22: Deflection basin of FEM	20
Figure 23: Hinge formation by (Panda & Ghosh, 2002a).....	20
Figure 24: Hinge formation developed by ANSYS model	21
Figure 25: Deflection variation along diagonal.....	21
Figure 26: Verification of ANSYS FEM by (Gunatilake & Mampearachchi, 2019)..	22
Figure 27: Block surface without cross beam	26
Figure 28: Loading position vs v.Deflection in (different laying patterns)	28

Figure 29: Loading position vs H. Deflection (different laying patterns)	29
Figure 30: Block surface with cross beam	30
Figure 31: Vertical deflection vs degree of slope	31
Figure 32: Horizontal deflection vs degree of slope	31
Figure 33: Combined graph of Vertical deflection vs degree of slope	32
Figure 34: Combined graph of Horizontal deflection vs degree of slope	32
Figure 35: 4m road section developed with ANSYS Workbench	33
Figure 36: Analysis of 4m road section	34
Figure 37: Cross beam intervals vs vertical deflection for different degree of slopes	38
Figure 38: Cross beam intervals vs vertical deflection for different degree of slopes	39

LIST OF TABLES

Table	Description	Page
Table 1:	Existing Concrete Block paved sloped roads	12
Table 2:	Section wised block paved sections	14
Table 3:	Material properties for SAP FEM (Mampearachchi & Gunarathna, 2010) .	17
Table 4:	Deflection variation along diagonal	22
Table 5:	Relative deflection of wheel path.....	24
Table 6:	Average deflection of wheel path of road section	26
Table 7:	FEM model analysis results.....	27
Table 8:	Vertical deflection vs degree of slope (Without cross beams)	28
Table 9:	Horizontal deflection vs. degree of slope	29
Table 10:	FEM model analysis results.....	30
Table 11:	Vertical deflection graphs from 0 ⁰ to 20 ⁰	36
Table 12:	Horizontal deflection graphs from 0 ⁰ to 20 ⁰	37

LIST OF ABBREVIATIONS

Abbreviation	Description
CBP	Concrete Block Paving
FEM	Finite Element Method
CB	Cross beam

1.0 INTRODUCTION

1.1. Background

Over the past few years, concrete block paving (CBP) has become a widely used solution for rural road construction due to its durability, ease of construction, and low maintenance requirements. It is particularly effective in areas with moderate to low traffic volumes, offering a cost-effective alternative to conventional asphalt or concrete pavements. CBP systems support regular maintenance without the need for expensive methods or advanced technologies, making them especially suitable for areas prone to frequent surface damage. Compared to traditional construction techniques which often face durability issues due to technical and environmental constraints and require higher financial investment CBP provides a more practical and economical solution (Panda & Ghosh, 2002a; Shackel, n.d.).

Nowadays, concrete block paving is being applied not only on flat terrain but also on steep slopes, primarily because of its cost efficiency and ease of implementation. The shape, size, and thickness of the paving blocks have been found to play a critical role in determining the performance and behavior of CBP systems, particularly on flat terrain.(Panda & Ghosh, 2002a). However, (Miura et al., n.d.) has indicated that, when rutting depth is used as a performance indicator, the shape of the paving blocks and the pattern in which they are laid have a greater influence on pavement performance than the thickness of the blocks. Finite element model analyses conducted by (Mampearachchi & Gunarathna, 2010) also demonstrated that the construction pattern plays a significant role in the overall performance of concrete block pavements (CBP).

It is important to note that the majority of previous studies have primarily focused on CBP applications in flat terrain conditions. But (Mudiyono, 2015) has done a laboratory-scale test to study the degree of slope, laying pattern, joint width, and thickness of paving block on the performance of CBP on slopes. While the herringbone 45° laying pattern with 3 mm joint width was observed to perform best on sloped sections, (Murat Algin, 2007) noted that pavers generally exhibit better performance when their laying pattern is aligned with, or perpendicular to, the direction of traffic ($\theta = 0^\circ$ or 90°). Even a slight deviation of 10° from these orientations can significantly reduce the effectiveness of interlock. Hence there are some contradictions among past

findings. Therefore it is needed to analyze how degree of slope affects in CBP in real ground situation.

1.2. Problem Statement

In the Concrete Block Pavement surfaces, three types of interlocking takes place concurrently to ensure optimal performance and durability as follows. (Mampearachchi & Senadeera, 2014);

- Vertical Interlocking.
- Rotational Interlocking.
- Horizontal interlocking.

Sand between joints helps in achieving vertical interlocking while transferring shear forces and rotational interlocking is achieved when adequately thick pavers are tightly laid and confined by edge restraints, such as curbs, which counteract lateral forces generated by vehicular movement. Specific laying patterns mainly helps in horizontal interlocking and the use of cross beams that help distribute forces generated by braking, turning, and accelerating vehicles. Curbs and cross beams play a crucial role in Concrete Block Pavement (CBP), as they help maintain horizontal interlock and ensure the integrity of the system under repeated lateral loads from traffic.

Unique challenges arise when constructing roads on steep slopes particularly due to the vertical traffic loads that also generate a surface component acting down slope on the paving blocks. These forces are further intensified by vehicle traction of accelerating uphill and braking forces from vehicles descending. Both of which contribute to significant horizontal loading on the pavement structure.

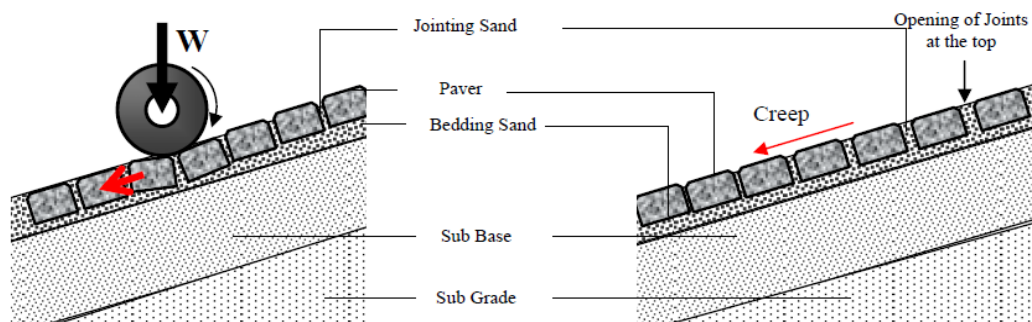


Figure 1: Deformation and horizontal creep of CBP for sloping road section (Mudiyono, 2015)

In most conventional pavements, these horizontal forces lead to the horizontal creep of blocks down slope, resulting in joint openings at the upper end of the pavement, rutting, and diminished riding quality.

Installing an anchor beam or cross beam at the lower end of the pavement can help mitigate this movement. However, it is also important to evaluate how other parameters such as block type, laying pattern, and laying angle affect the extent of this creep. Understanding these influences is essential for determining the maximum permissible slope for block paving in rural roads.

2.0 OBJECTIVES

This research aims to achieve the following objectives.

- To investigate the site conditions related to the laying of concrete block paving on steep slopes in rural roads.
- To determine how the shape of concrete blocks, laying pattern, and laying angle affect pavement performance with respect to the degree of slope, based on both field observations and FEM modeling.
- To identify the role of external supports (e.g., cross beams) and to determine the optimum spacing of such supports to minimize creep in sloped road sections.

3.0 LITERATURE REVIEW

3.1. Effect of laying pattern

Complicated stress distributions can be identified in Concrete Block Pavement (CBP) surfaces due to the interconnection action between blocks, which makes challenging work to accurately assess stress variations under field conditions. However, identifying an effective laying pattern that enhances interlocking is crucial. Models created using three dimensional software such as SAP2000, provides the capability to evaluate the performance comparison of various laying patterns which is challenging to assess in the field. According to the model, the herringbone bond pattern exhibits smaller vertical deflection, while the stack bond pattern exhibits greater deflection. This suggests that the herringbone bond pattern offers greater stability under vertical loading. (Mampearachchi & Gunarathna, 2010)

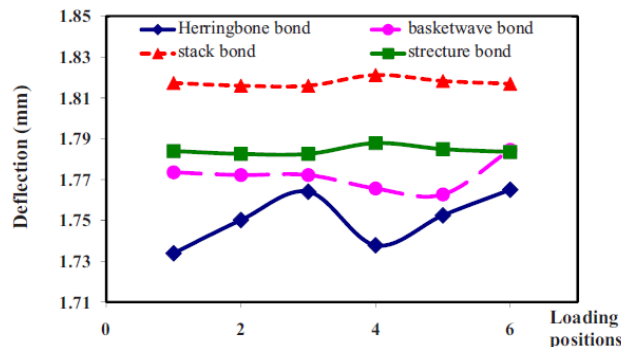


Figure 2: Loading positions vs vertical deflection(different laying patterns)

As shown in Figures 2 and 3, vertical deflection is greater than horizontal deflection (nearly 3 times) and no significant difference in horizontal deflection among laying patterns. Therefore, when selecting a strong bond pattern under braking effects, the vertical deflection curve can be considered as the key factor. Considering vertical loading and braking forces, the herringbone bond pattern exhibits the lower deflection and demonstrates superior interlocking performance. Consequently, for improved structural integrity, the herringbone bond pattern is advised in road construction projects.

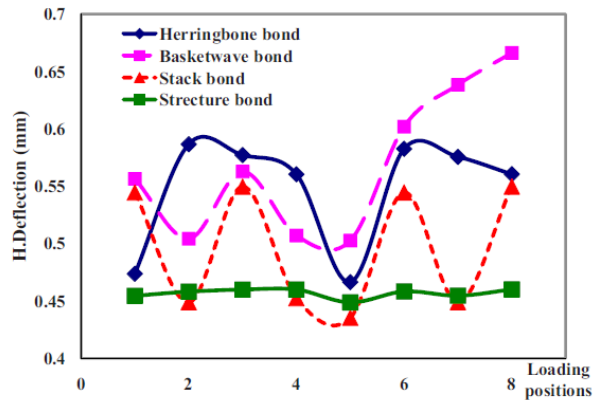


Figure 3: Loading position vs H. deflection (Different laying patterns)

(Mudiyono, 2015; Murat Algin, 2007) conducted a laboratory setup with steel frame to analyze these parameters. Herringbone 45°, herringbone 90°, and stretcher bond as well as different joint widths (3, 5, 7mm) were included in the laboratory setup. Results were evaluated horizontal creep and deflection wise under a load equivalent to 0.5 times of allowable single axle limit.

It was found that pavements laid in a stretcher bond pattern did not fully develop interlock. In fact, as the wheel load increases these pavements failed along the joints. But concrete block pavers laid in a herringbone bond achieved overall interlock and resisted wheel loads up to 51 kN. These findings suggest that herringbone bond patterns provide superior performance compared to the stretcher bond under similar loading conditions.

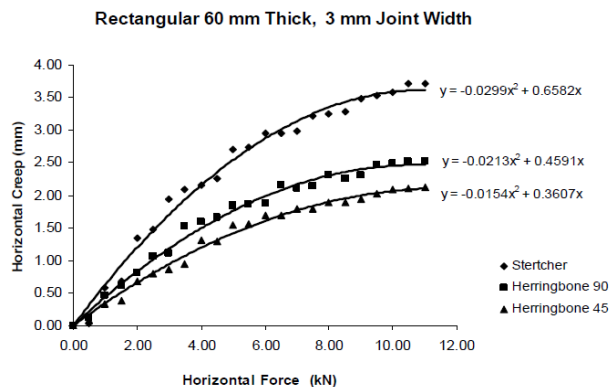


Figure 4: Horizontal force vs Horizontal creep to analyze the effect of laying pattern

3.2. Effect of Block shape

According to (Mampearachchi & Senadeera, 2014), A 100-meter road segment was selected and divided into 10 equal sections. In each section, concrete blocks were laid using different block shapes and patterns. Surface deflection and displacement of blocks were measured using Benkelman beam deflectometer and vernier caliper respectively as described in a early study on finite element model (FEM) analysis.

Figure 5 presents the maximum deflections for three types of concrete blocks. The laying angle was maintained at 90°, and the stretcher bond pattern was used consistently across all sections. Among the block types, the Uni-style block exhibited the lowest deflection, while the Keystone & Cobble blocks showed comparatively higher deflections.

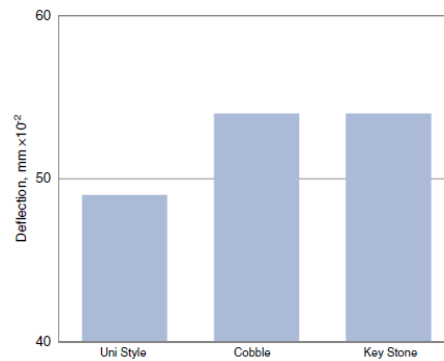


Figure 5: Effect of block shapes on deflection

Figure 6 illustrates distinct deflection patterns for different block shapes: cobble blocks produce a narrow, deep deflection basin, while uni-style blocks result in a broader, shallower basin. This behavior can be attributed to the greater vertical surface area of uni-style blocks compared to cobble or keystone shapes, which increases the contact area for frictional interaction with adjacent units. It can be inferred that the capacity for load transfer between blocks is closely related to the extent of their vertical interface.

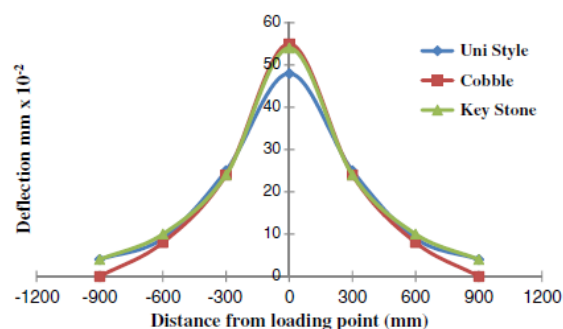


Figure 6: Loading point vs deflection (deflection profile)

3.3. Effect of laying angle

In studies by (Mampearachchi & Senadeera, 2014), three different laying angles were selected to evaluate the effect of orientation on pavement performance. Field tests were conducted using a consistent laying pattern (stretcher bond) and block shape (Uni-style). The results showed that laying angles of 0° and 90° produced the least deflection, whereas 45° angle resulted in significantly higher deflection under wheel loading.

45° angle at the wheel load recorded maximum deflection and a narrow, deep deflection basin was observed at this angle, while shallow and wider deflection basins were associated with the 0° and 90° orientations. The wider, shallow deflection profiles at 0° and 90° suggests load transferring between adjacent blocks more effective. Hence it is concluded that laying blocks at 0° or 90° angles promotes better interlock and load distribution, resulting in lower deflection at the center.

But according test results of (Mudiyono, 2015; Murat Algin, 2007), horizontal creep is lower herringbone 45°. Hence blocks laid in herringbone 45° performed better than herringbone 90°

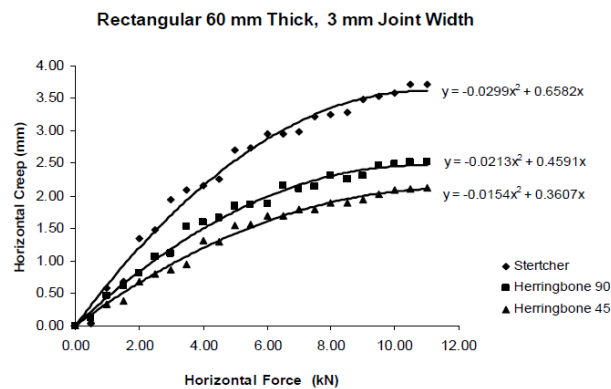


Figure 7: The effect of laying angle

According to laboratory-scale test done by (Mudiyono, 2015; Murat Algin, 2007), effect of joint width, paver thickness and effect of degree of slope was analyzed as follows.

3.4. Effect of joint width

In all these experiments, a 50 mm loose thickness of sand was used for the bedding course. The results indicate that a decrease in joint width leads to a corresponding reduction in pavement deflection.

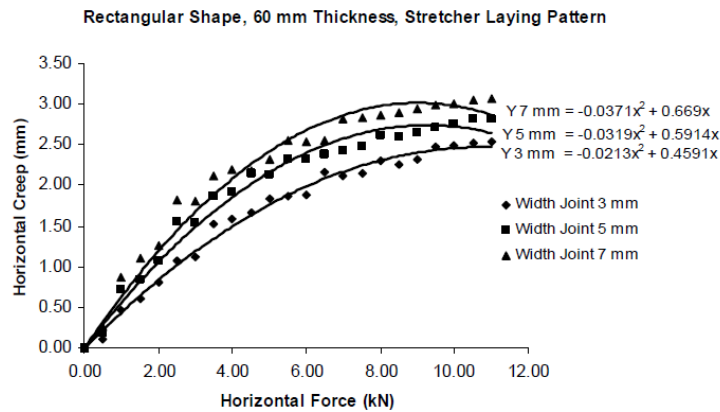


Figure 8: Horizontal force vs Horizontal creep(effect of width of joints)

3.5. Effect of paver thickness

Two thicknesses of paving (60 & 100 mm) were used to evaluate pavement response and results showed that increasing the thickness of the paving blocks reduced both horizontal creep and block uplift. This improvement is attributed to the increased contact area between thicker blocks, which enhances frictional resistance and interlock between adjacent blocks.

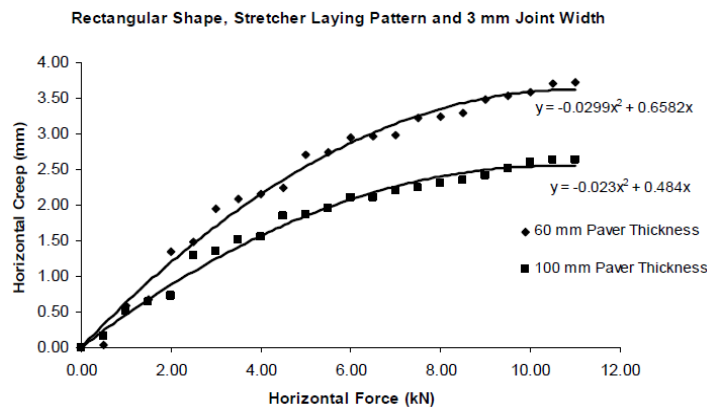


Figure 9: Horizontal force vs Horizontal creep (The effect of thickness of paving)

3.6. Effect of degree of the slope

The results of the full-scale laboratory experiment, as illustrated in Figure 10, indicate that increasing the slope leads to greater horizontal creep while reducing vertical displacement. This behavior can be attributed to the expansion of the contact area between blocks on steeper slopes, which enhances frictional resistance and limits vertical movement.

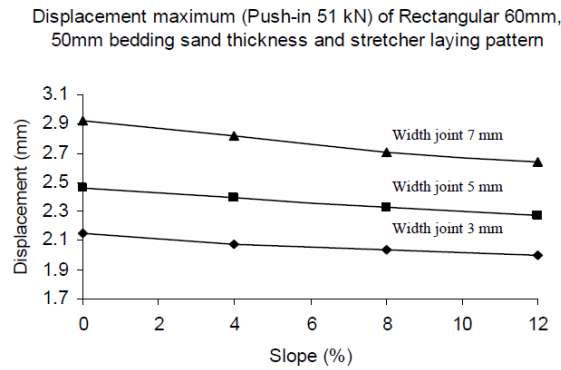


Figure 10: The effect degree of slope

There are some contradictions among literature and most of the findings are on flat terrains. Therefore it is needed to analyze how degree of slope affects in CBP in real ground situation.

3.7. Effect of cross beams

As per the “Concrete block paving technical note for steel slopes” published by Concrete Manufactures Association of South Africa, to prevent the horizontal creep of the blocks down the road, it has recommended anchor beams shall be placed in between interlock paving where the slope is greater than 12%. If the slope is between 8% and 12% anchor beams should be used at the discretion of the engineer.

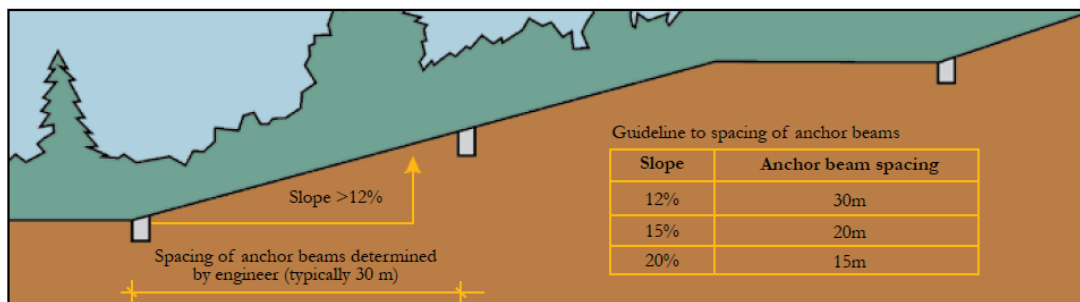


Figure 11: Sloping of anchor beams

4.0 METHODOLOGY

4.1. Monitoring of existing block paved roads in sloped sections

Nowadays Concrete Block Paving (CBP) is a widely used surfacing technique for rural roads in Sri Lanka. In earlier times, concrete paving was typically used for roads in sloped terrains. However, due to its cost-effectiveness and ease of construction, block paving has now become commonly used even on steep slopes.



Figure 12: 12° sloped block paved road

In common practice, Concrete Block Paving (CBP) is implemented in various block patterns across different slope conditions. This variation is primarily due to the fact that rural roads are owned and maintained by divisional councils, and there are currently no standardized guidelines for the construction of block-paved roads. As a result, inconsistent construction practices can be observed across rural roads. Some of the commonly seen block paving practices are as follows.





Road	Slope	Block type	Block Pattern & Angle	Cross beam availability
	6°	Uni-Style	Herring bone 0°/90°	Yes
	4°	Uni-Style	Herring bone 45°	Yes
	10°	Uni-Style	Herring bone 45°	No
	12°	Uni-Style	Herring bone 0°/90°	No

Table 1: Existing Concrete Block paved sloped roads

Table 1 presents some of the sloped road sections observed during field inspections. These four road sections represent four different construction types. The only common feature among them is the use of Uni-style blocks. Considering block laying patterns, some road sections use a herringbone $0^{\circ}/90^{\circ}$, while some use herringbone 45° .

Another key difference observed was the presence and quality of cross beams. In some sloped road sections, no cross beams were provided, and in others, the existing cross beams were non-standard. In most cases, during block laying, a gap is left every 20–30 meters, and concrete is simply poured into these spaces, without proper structural detailing.



Figure 13: Common field practice of placing cross spacing

As per the “Concrete block paving technical note for steel slopes” standard method of placing cross beams are as follows

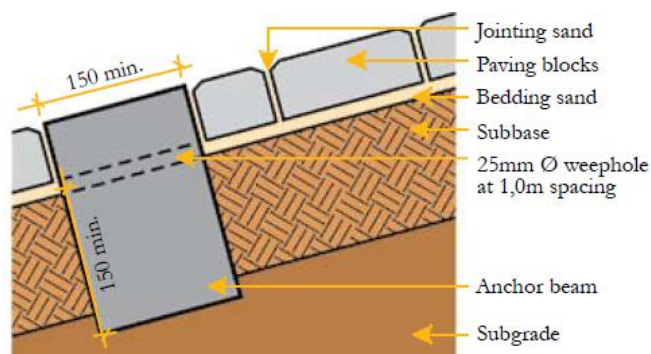


Figure 14: Standard method of placing cross beams

4.2. Developing trail concrete block surface

A 90-meter long gravel subgrade road section with a varied slope ranging from 0% to 10% was selected for the trial. The subgrade was compacted using a 10-ton roller, and the base was prepared using a 150 mm thick aggregate base course. A 50 mm thick quarry dust layer was used as the bedding layer, which was leveled with a leveling stick and compacted using a plate compactor.

Road sections of 5 meters and 10 meters in length were selected, and Uni-style blocks were placed manually, with varying block patterns. The edge restraints and cross beams were constructed after the placement of the blocks.



Figure 15: Block placing in trail section

Chainage	Road section length	Pattern	Cross beam availability
0+000-0+012	12m	Herringbone 90 ⁰	Yes
0+012-0+020	8m	Herringbone 90 ⁰	Yes
0+020-0+030	10m	Herringbone 45 ⁰	Yes
0+030-0+040	10m	Stretcher bond	Yes
0+040-0+050	10m	Herringbone 90 ⁰	Yes
0+050-0+056	6m	Herringbone 90 ⁰	No
0+056-0+062	6m	Herringbone 90 ⁰	No
0+062-0+072	10m	Herringbone 90 ⁰	Yes
0+072-0+078	6m	Herringbone 45 ⁰	Yes
0+078-0+082	4m	Herringbone 90 ⁰	Yes
0+082-0+090	8m	Herringbone 90 ⁰	Yes

Table 2: Section wised block paved sections



Figure 16: Finished trial block paved road section

4.3. Analysis of Field data

After completing the block paving deflection of the wheel path of the surface was taken before allowing the traffic



Figure 17: Identification of wheel path in completed trail road section

Automatic level was used to get the levels of the wheel path after construction. Then after 6 months of construction, levels of the wheel path was taken and relative deflection was calculated.



Figure 18: Surface level checking using Automatic level instrument

Surface levels of the wheel path (LHS & RHS) was taken 2m intervals as shown in Appendix A-1

After 6 months of construction, surface levels of same points of wheel path which was taken earlier were again measured using automatic level as shown in Appendix A-2

4.4. Finite Element modelling of CBP

SAP FEM was initially developed to analyze support conditions, specifically the base and sub grade layers. However, due to limitations in the SAP2000 software, it is not suitable for analyzing different block shapes and laying patterns. Therefore, ANSYS Workbench was selected to develop a similar three-dimensional (3D) model, allowing for more advanced analysis of block shapes and patterns, particularly under sloped conditions. In this study, it was assumed that the subgrade had a uniform effect on pavement deflection across all types of block shapes and laying patterns. (Gunatilake & Mampearachchi, 2019). As the main objective was to evaluate deflection and stress differences between various block configurations and patterns, the subgrade's

influence was considered consistent and therefore not included in the finite element model (FEM). As a result, the FEM focused solely on modeling the block layer, the sand bedding layer, and the aggregate base course (ABC) layer.

4.5. ANSYS Workbench for finite Element model analysis

The cobble block pavement geometry was constructed directly within ANSYS Workbench. In contrast, for more complex shapes like the Uni-style block, the geometry was initially designed in SolidWorks and subsequently imported into ANSYS Workbench. The finite element model (FEM) utilized higher-order 3D solid elements with 20 nodes, which are capable of capturing quadratic displacement behavior. To enhance solution precision and ensure better convergence, the Hexa Dominant meshing approach was applied.

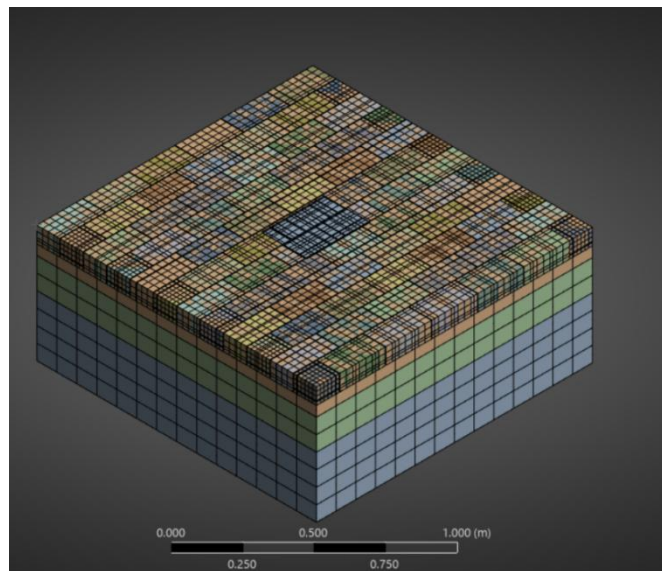


Figure 19: Mesh developed in ANSYS Workbench

The concrete blocks, sand, and road base materials were modeled as isotropic and linearly elastic. Their mechanical behavior was defined using parameters such as elastic modulus, Poisson's ratio, and shear modulus, as summarized in Table 5.

Material	Modulus of elasticity (E)(GPa)	Poisson's ratio	Shear modulus (G)(GPa)
Concrete	23.2	0.20	9.667
Sand	0.01	0.26	0.00396
ABC	0.24	0.30	0.0923
Soil	0.12	0.40	0.0429

Table 3: Material properties for SAP FEM (Mampearachchi & Gunarathna, 2010)

Identical material properties were applied to both the bedding sand and filling sand, as the compaction effect on their behavior was deemed insignificant. The filling sand was represented as a slab containing voids that matched the dimensions and geometry of the concrete blocks. These blocks were then inserted into the voids and considered to be bonded with the surrounding filling sand. The contact between the concrete blocks and the filling sand was modeled as fully bonded, with the properties of the filling sand explicitly defined within the simulation. This modeling technique aligns with previously validated approaches used in earlier studies to simulate sand-filled joints. (Gunatilake & Mampearachchi, 2019; Mampearachchi & Gunarathna, 2010). Thermal effects, such as contraction and expansion of concrete due to temperature variations, were excluded from the analysis since the pavement system comprised small, discrete units not exceeding 200 mm. The finite element model (FEM) incorporated the filling sand, bedding sand, base course, and concrete pavers. The model's dimensions were derived from the experimental setup and the SAP FEM configuration employed by (Mampearachchi & Gunarathna, 2010).

- ABC layer: 200mm
- Sand bedding: 40mm
- Sand filling: 5mm
- Concrete block: 210mm x 100mm x 75mm

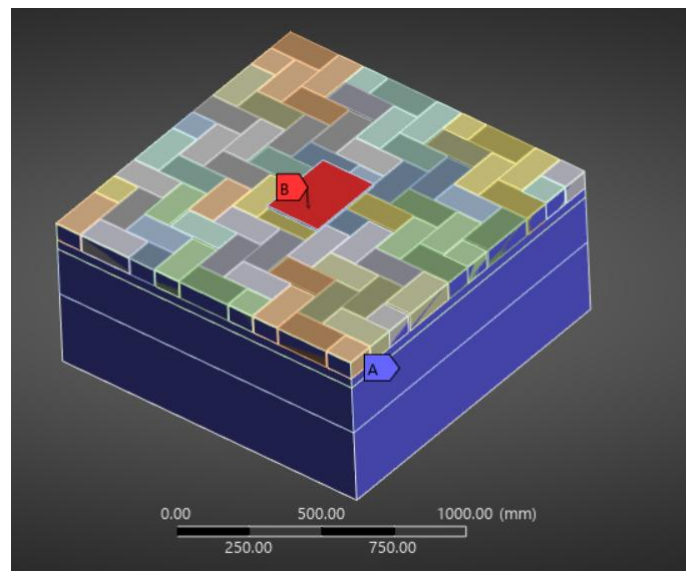


Figure 20: Geometry developed with ANSYS Workbench

In the study by (Mampearachchi & Gunarathna, 2010) a point load of 60 kN was applied over a rectangular area of 310 mm × 225 mm at the center of the model, simulating the tire contact area of a single wheel (Panda & Ghosh, 2002a). This same loading approach was adopted in the present model, with a 60 kN load distributed across the same contact area. To replicate realistic boundary conditions, the bottom surface of the model was fully constrained in all directions, preventing any displacement. Meanwhile, the pavement's four lateral boundaries were restricted from moving horizontally but were allowed vertical movement, effectively mimicking the confinement typically provided by curbs. In order to model the surface slope condition, inclined load was divided into vertical and horizontal load components (Figure 21) considering slope angle starting from 0°. As per the Geometric design standards of roads published by Road Development Authority, mountainous terrains are classified as corridor slope more than 25% which is around 15°. Hence for this analysis maximum degree of slope has taken as 20° which is a steeper slope value for rural roads. The other main surface load is the frictional force acting on the surface due to the vehicle movement. Friction coefficient taken as the 0.8 for concrete surfaces and when vehicle movements are into upwards highest horizontal force is applied on the surface due to the load component and the frictional force.

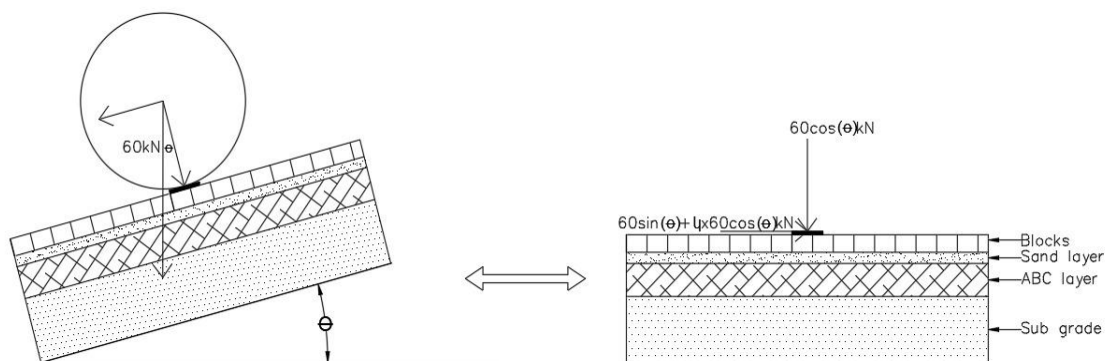


Figure 21: Load application as horizontal and vertical components

4.6. Validation of the ANSYS Finite Element model

The accuracy of the ANSYS finite element model (FEM) was validated by comparing its deflection basin results with data from both a laboratory model and the SAP model developed in an earlier study by (Mampearachchi & Gunarathna, 2010). For consistency, the comparison was based on the setup referred to as Test 4 in that study, as it closely matched the support conditions and loading arrangement implemented in the ANSYS finite element model.

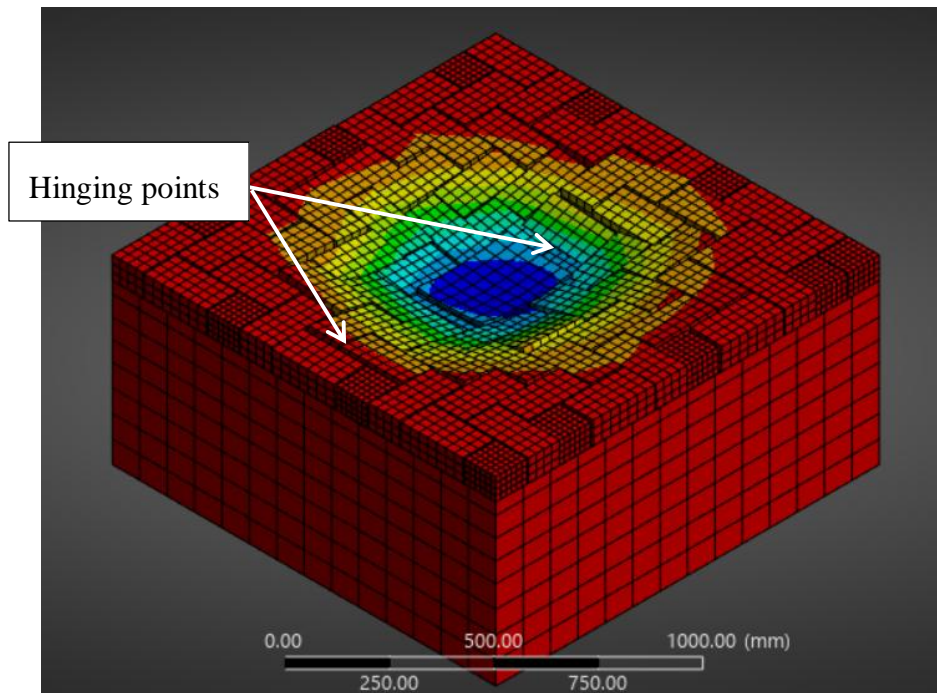


Figure 22: Deflection basin of FEM

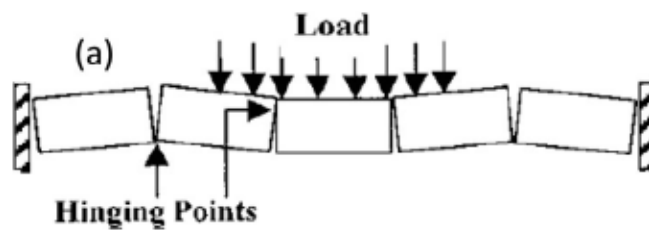


Figure 23: Hinge formation by (Panda & Ghosh, 2002a)

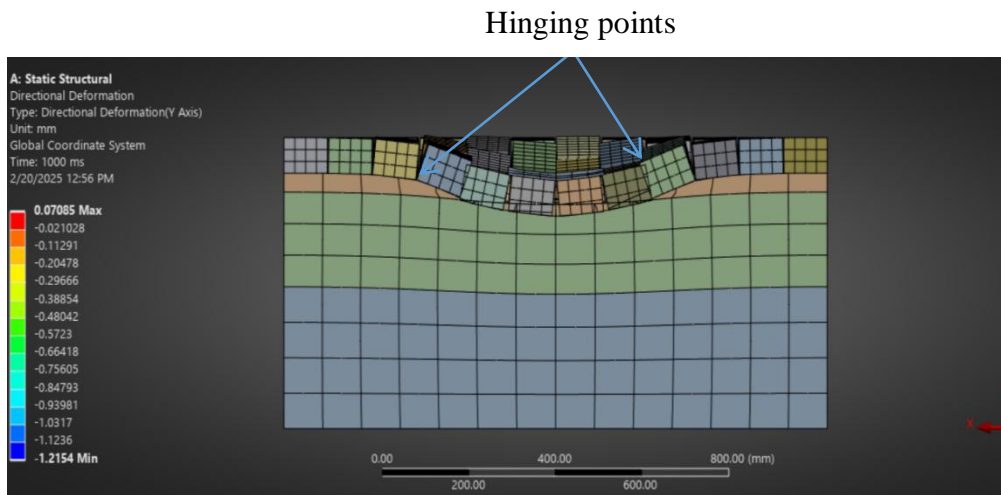


Figure 24: Hinge formation developed by ANSYS model

The hinging behavior, initially identified by (Panda & Ghosh, 2002a) and illustrated in Figure 23, describes how hinges develop at different locations depending on block positioning relative to the applied load. Specifically, blocks directly under the load exhibited hinge formation at their upper edges, while neighboring blocks developed hinges at their lower edges. Minimal joint gaps were observed at these hinge points, with wider gaps occurring at the opposite ends. This observed behavior supports the validity of the joint representation method used in the current finite element model (FEM). To further verify the model, deflection patterns were also examined along the diagonal axis.

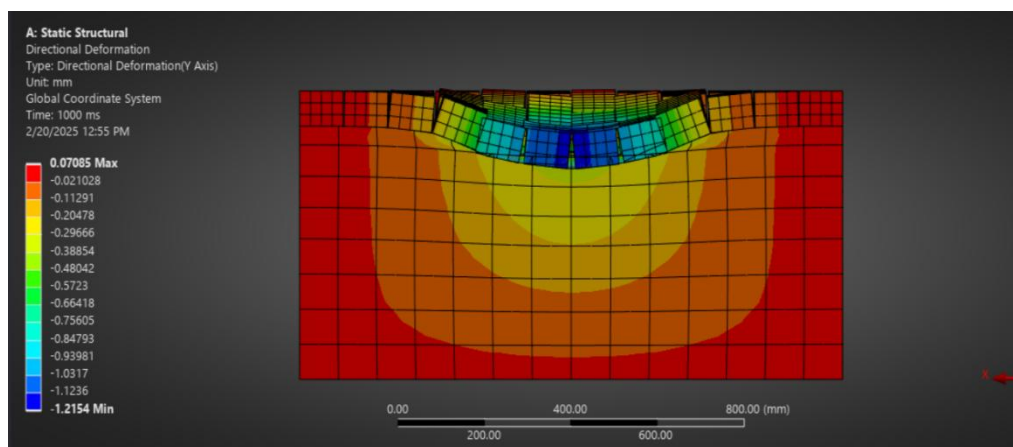


Figure 25: Deflection variation along diagonal

As observed in earlier research, the greatest deflection occurred directly beneath the point of load application (Table 6). Figure 26 presents a comparison of the deflection basins derived from the laboratory setup, the SAP model developed by (Mampearachchi & Gunarathna, 2010) and the ANSYS model used by (Gunatilake & Mampearachchi, 2019). The ANSYS finite element model (FEM) produced comparable deflection patterns, reinforcing its effectiveness in simulating the behavior of concrete block pavements.

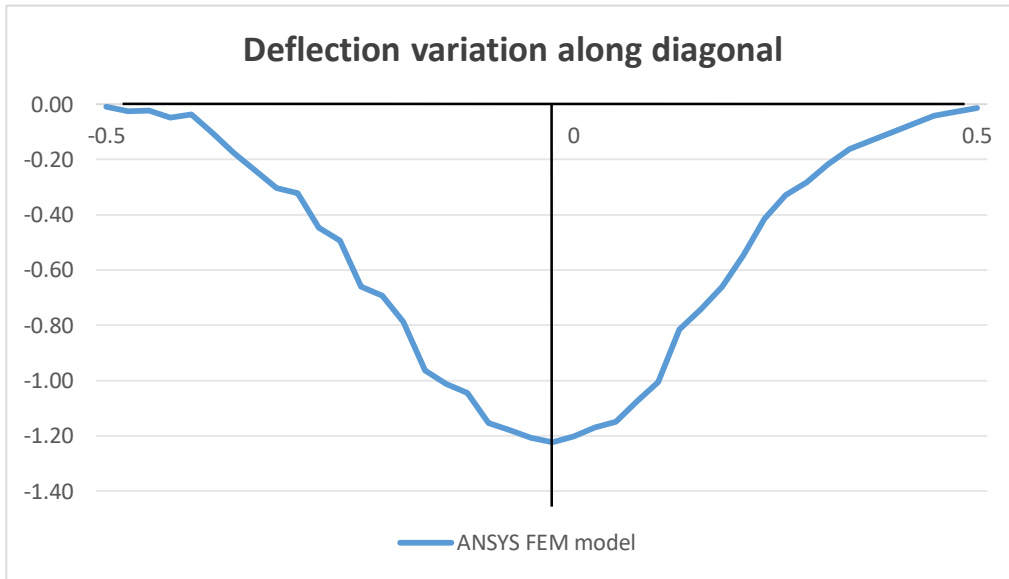


Table 4: Deflection variation along diagonal

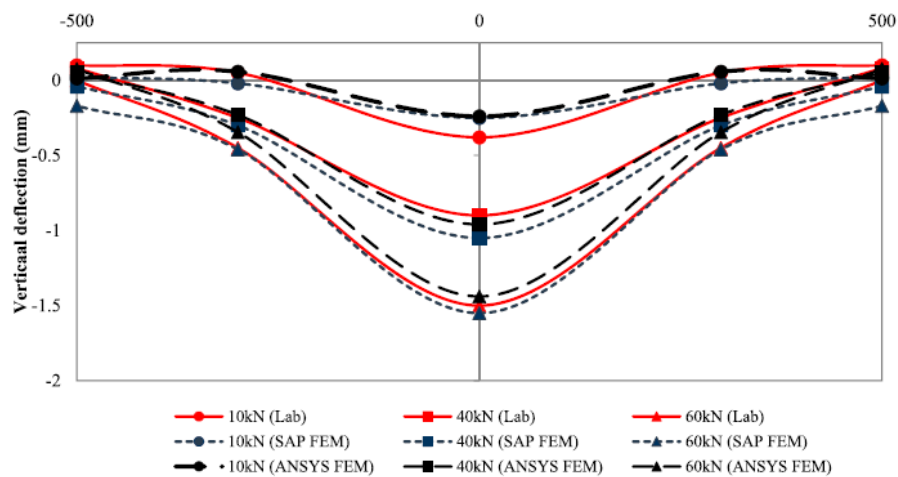


Figure 26: Verification of ANSYS FEM by (Gunatilake & Mampearachchi, 2019)

Based on the findings above, the ANSYS FEM was employed for further analysis to determine the maximum permissible slope for block paving on rural roads.

5.0 RESULTS AND ANALYSIS

5.1. Outcomes of developed trail Concrete block surface

Relative deflection of the wheel path was taken as the difference between the surface levels of the same points of the wheel path before allowing traffic and 6 months after allowing traffic.

Chainage	Relative Vertical Deflection of wheel path (mm)	
	LHS	RHS
0+000	-0.002	-0.003
0+002	-0.001	-0.002
0+004	-0.002	-0.003
0+006	-0.001	-0.003
0+008	-0.003	-0.002
0+010	-0.003	-0.004
0+012	-0.002	-0.004
0+014	-0.004	-0.003
0+016	-0.001	-0.003
0+018	-0.004	-0.004
0+020	-0.003	-0.002
0+022	-0.005	-0.004
0+024	-0.003	-0.003
0+026	-0.002	-0.004
0+028	-0.003	-0.004
0+030	-0.005	-0.005
0+032	-0.002	-0.003
0+034	-0.003	-0.003
0+036	-0.002	-0.001
0+038	-0.003	-0.004
0+040	-0.004	-0.004
0+042	-0.003	-0.002
0+044	-0.005	-0.004
0+046	-0.003	-0.003
0+048	-0.002	-0.004
0+050	-0.003	-0.003
0+052	-0.002	-0.004

0+054	-0.003	-0.004
0+056	-0.005	-0.005
0+058	-0.003	-0.004
0+060	-0.002	-0.004
0+062	-0.004	-0.003
0+064	-0.001	-0.003
0+066	-0.004	-0.004
0+068	-0.003	-0.002
0+070	-0.005	-0.004
0+072	-0.003	-0.003
0+074	-0.002	-0.004
0+076	-0.002	-0.004
0+078	-0.003	-0.003
0+080	-0.002	-0.004
0+082	-0.003	-0.004
0+084	-0.005	-0.005
0+086	-0.003	-0.004
0+088	-0.002	-0.004
0+090	-0.004	-0.003

Table 5: Relative deflection of wheel path

Average deflection of the wheel path of road section was calculated as follows.

Chainage	Bond type & Angle	LHS Avg Vertical Deflection (mm)	RHS Avg Vertical Deflection (mm)
0+000	Herringbone 90 ⁰	-0.002	-0.003
0+002			
0+004			
0+006			
0+008			
0+010			
0+012			
0+014	Herringbone 90 ⁰	-0.003	-0.003
0+016			

0+018			
0+020			
0+022	Herringbone 45 ⁰	-0.004	-0.004
0+024			
0+026			
0+028			
0+030			
0+032	Stretcher Bond	-0.003	-0.003
0+034			
0+036			
0+038			
0+040			
0+042	Herringbone 90 ⁰	-0.003	-0.003
0+044			
0+046			
0+048			
0+050			
0+052	Herringbone 90 ⁰	-0.003	-0.004
0+054			
0+056			
0+058	Herringbone 90 ⁰	-0.003	-0.004
0+060			
0+062			
0+064	Herringbone 90 ⁰	-0.003	-0.003
0+066			
0+068			
0+070			
0+072			
0+074	Herringbone 45 ⁰	-0.002	-0.004
0+076			
0+078			
0+080	Herringbone 90 ⁰	-0.003	-0.004
0+082			
0+084			

0+086			
0+088			
0+090			
	Average vertical Deflection of wheel path	-0.003	-0.004

Table 6: Average deflection of wheel path of road section

From Table 8 it is observed that average vertical deflection of the wheel path varies from mm to 4mm and there is no much effect on the bond type or laying angle. Horizontal deflection was not measured in this trail section.

5.2. Outcomes of FEM Model

An ANSYS model was developed for two types of block patterns: Herringbone and Stretcher Bond. To simulate the surface slope condition, an inclined load was applied by decomposing it into vertical and horizontal components based on slope angles ranging from 0° to 15°. To analyze the effect of cross beams, two sets of models were created: one with cross beams and one without cross beams. These models were further varied based on block pattern, block laying angle, and slope gradient to evaluate their impact on pavement performance.

5.2.1. Road section without cross beams

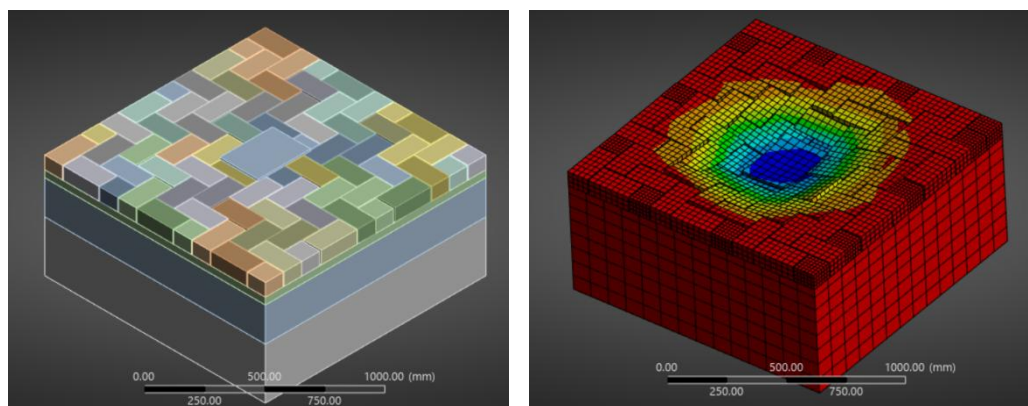


Figure 27: Block surface without cross beam

Above models were developed without cross beams and analysis results were generated as follows (Table 9).

Description			Without Cross beams	
Block Pattern	Angle (deg)	Slope(deg)	Vertical Deflection(mm)	Horizontal deflection(mm)
Herringbone Bond	0-90	0	1.100	0.290
		5	1.090	0.330
		10	1.080	0.350
		15	1.070	0.370
		20	1.063	0.392
	45	0	1.151	0.378
		5	1.139	0.389
		10	1.129	0.398
		15	1.119	0.400
		20	1.109	0.409
Stretcher Bond	0-90	0	1.201	0.172
		5	1.185	0.212
		10	1.170	0.252
		15	1.163	0.291
		20	1.153	0.330
	45	0	1.245	0.24
		5	1.242	0.246
		10	1.229	0.278
		15	1.206	0.325
		20	1.189	0.386

Table 7: FEM model analysis results

Using FEM model results graphs were developed for vertical deflection & horizontal deflection against degree of slope. According to 3D software model, herringbone pattern gave lower vertical deflection value while stretcher bond pattern gave the higher deflection.

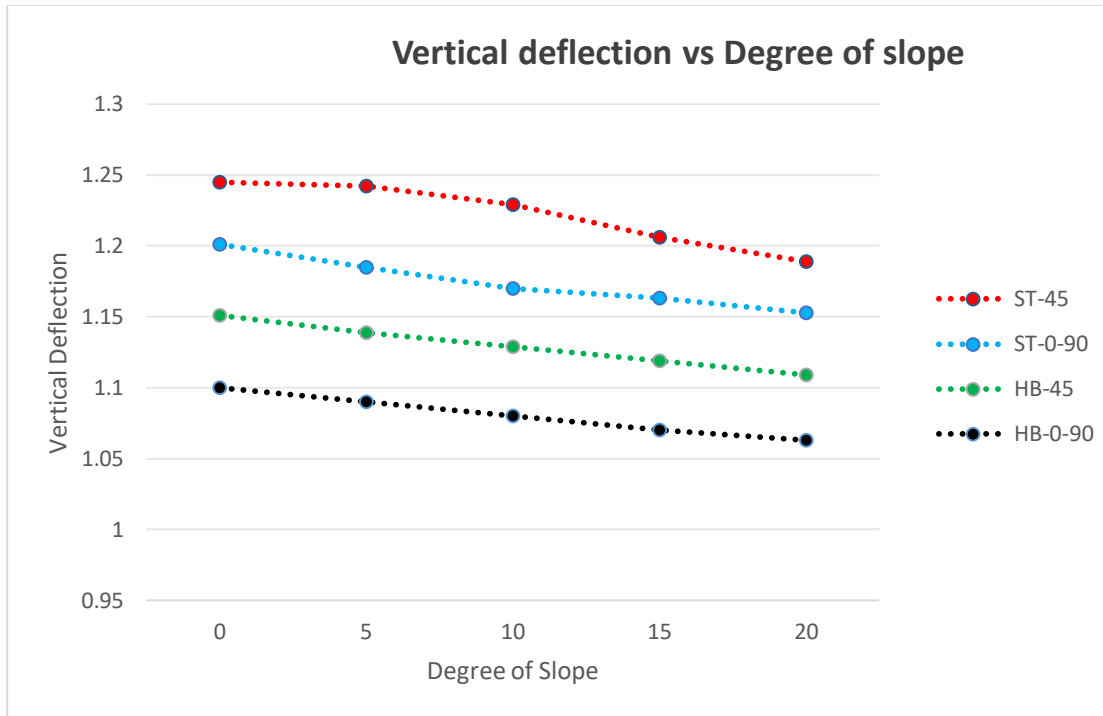


Table 8: Vertical deflection vs degree of slope (Without cross beams)

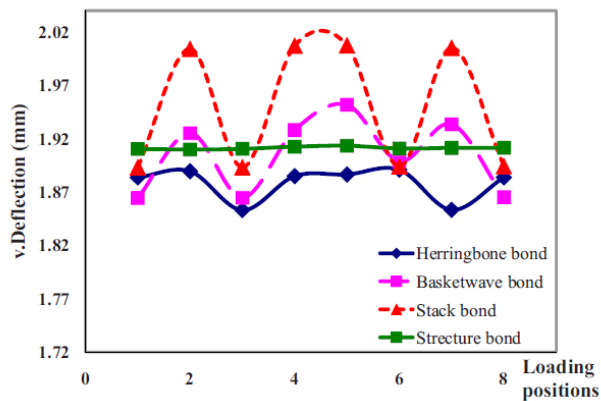


Figure 28: Loading position vs v.Deflection in (different laying patterns)

Same scenario was observed in (Mampearachchi & Gunarathna, 2010) when analyzing the effective laying pattern (Figure 29). The Herringbone pattern exhibited the lowest vertical deflection, while the Strecture Bond pattern resulted in the highest deflection. Among the herringbone configurations, the 0° – 90° laying angle showed less vertical deflection compared to the 45° angle. For the Strecture Bond, both laying angles produced similar deflection outcomes.

Across all four laying configurations, a common trend was observed. As the degree of slope increased, the vertical deflection decreased. This is primarily because, with increasing slope, a portion of the vertical load is redistributed along the inclined surface, resulting in a reduced effective vertical load acting perpendicular to the pavement surface.

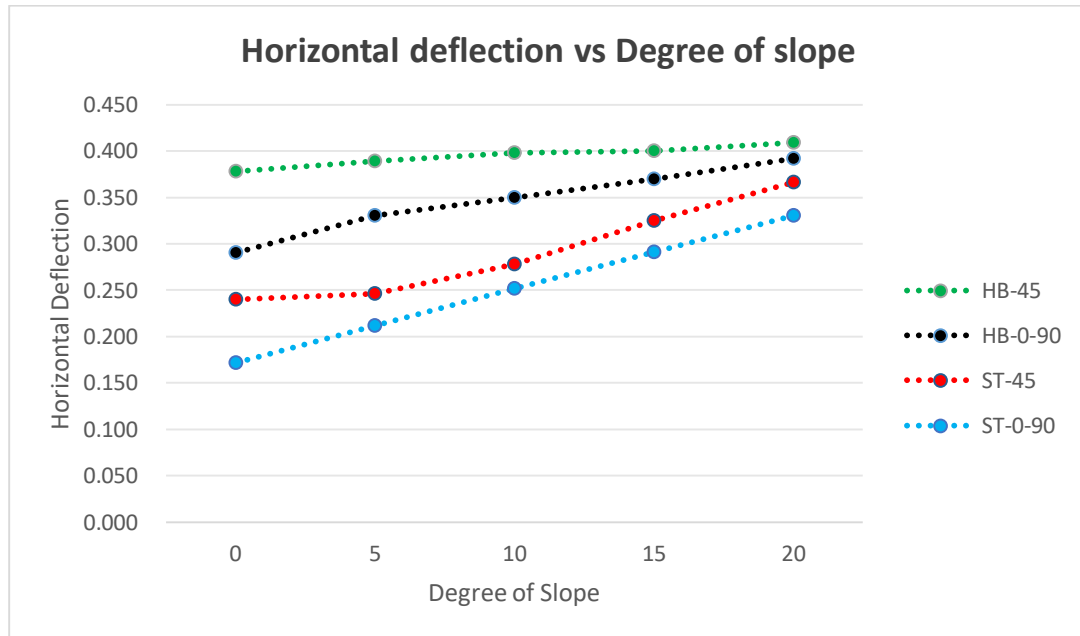


Table 9: Horizontal deflection vs. degree of slope

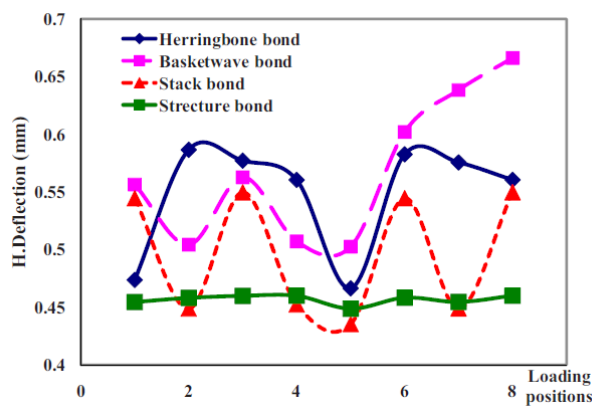


Figure 29: Loading position vs H. Deflection (different laying patterns)

In (Mampearachchi & Gunarathna, 2010), least deflection in horizontal direction observed in stretcher bond pattern and higher horizontal deflection observed in herringbone pattern.(Figure 31). A similar outcome was observed in the FEM analysis for horizontal deflection, where the Stretcher Bond pattern at 45° exhibited the least horizontal deflection, while the Herringbone pattern at 45° showed the largest

deflection. In all cases, a common trend was that horizontal deflection increased with the degree of slope. This increase is attributed to the growing horizontal load component generated by the slope angle.

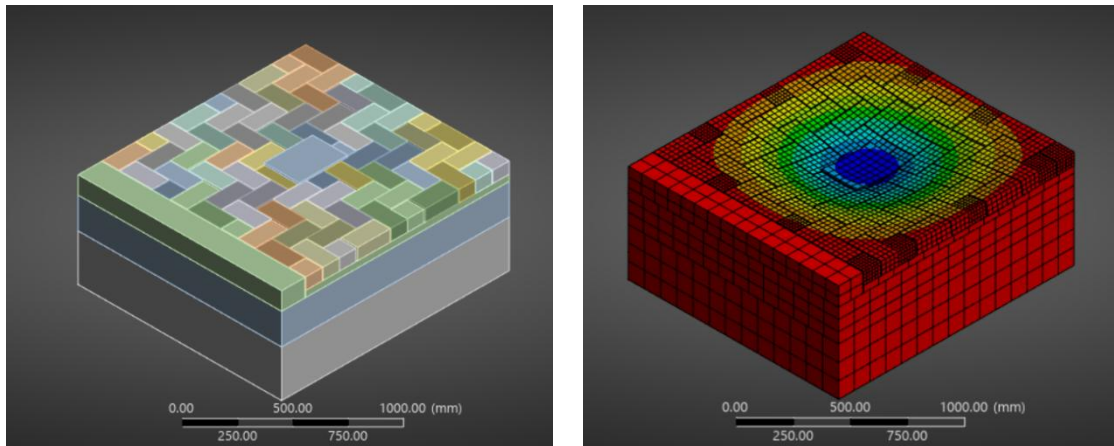


Figure 30: Block surface with cross beam

FEM model was generated including cross beam and analysis results were generated as follows (Table 9).

Description			With Cross beams	
Block Pattern	Angle (deg)	Slope(deg)	Vertical Deflection(mm)	Horizontal deflection(mm)
Herringbone Bond	0-90	0	0.496	0.037
		5	0.484	0.040
		10	0.468	0.042
		15	0.458	0.044
		20	0.448	0.045
	45	0	0.512	0.037
		5	0.500	0.039
		10	0.492	0.041
		15	0.480	0.042
		20	0.470	0.043
Stretcher Bond	0-90	0	0.516	0.035
		5	0.507	0.037
		10	0.495	0.038
		15	0.485	0.041
		20	0.477	0.042
	45	0	0.518	0.033
		5	0.515	0.034
		10	0.501	0.037
		15	0.491	0.039
		20	0.483	0.040

Table 10: FEM model analysis results

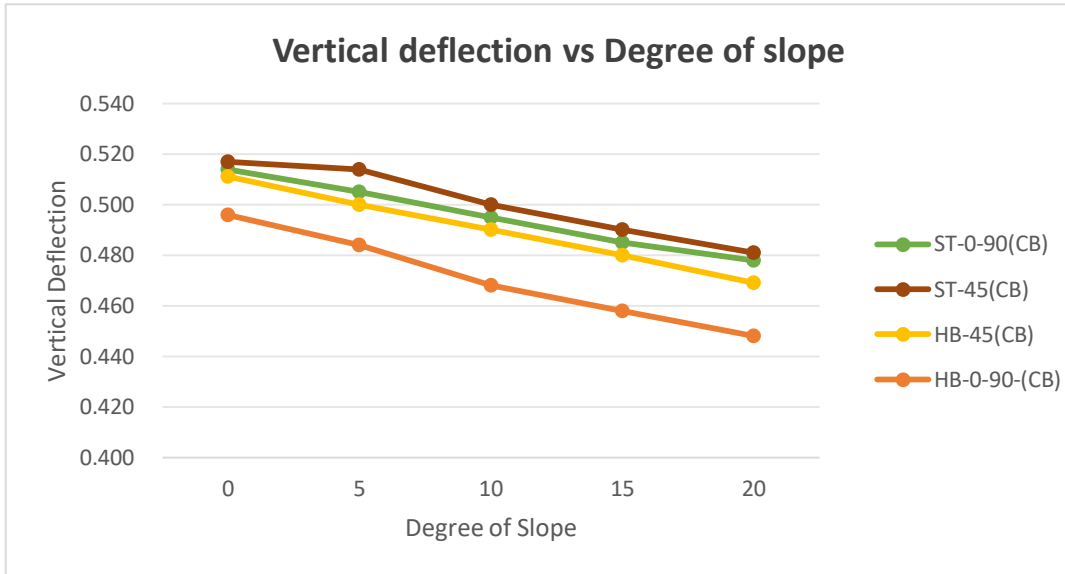


Figure 31: Vertical deflection vs degree of slope

With the introduction of cross beam, the vertical deflection was reduced from 1.10 mm to 0.51 mm, nearly halving the original value. Additionally, vertical deflection decreased with increasing slope angle in all cases.

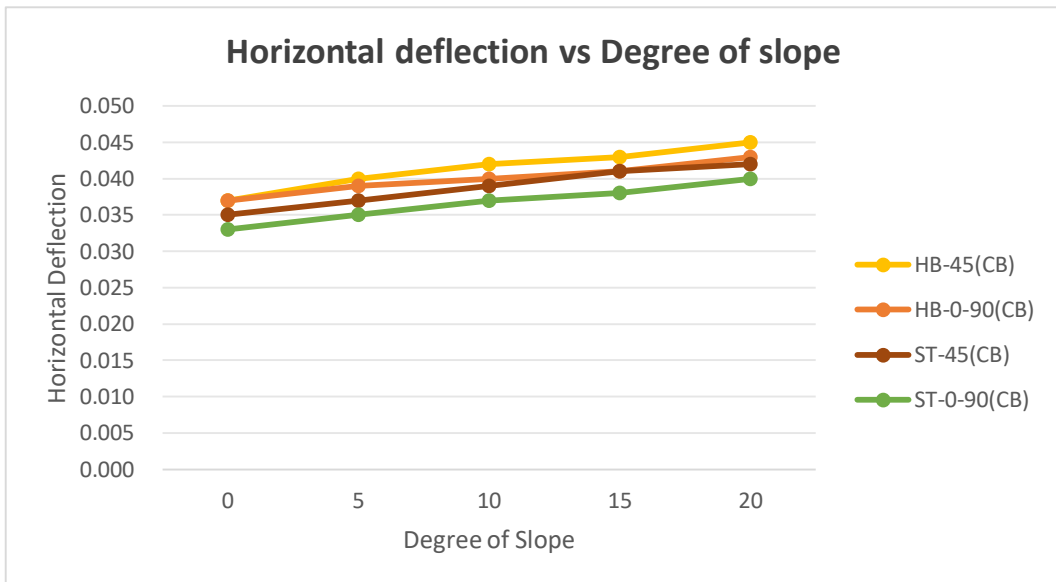


Figure 32: Horizontal deflection vs degree of slope

Horizontal deflection showed a significant reduction with the introduction of cross beams, dropping from 0.3 mm to 0.035 mm, which is almost ten times smaller. This clearly demonstrates the substantial impact of cross beams on the stability of concrete block surfaces.

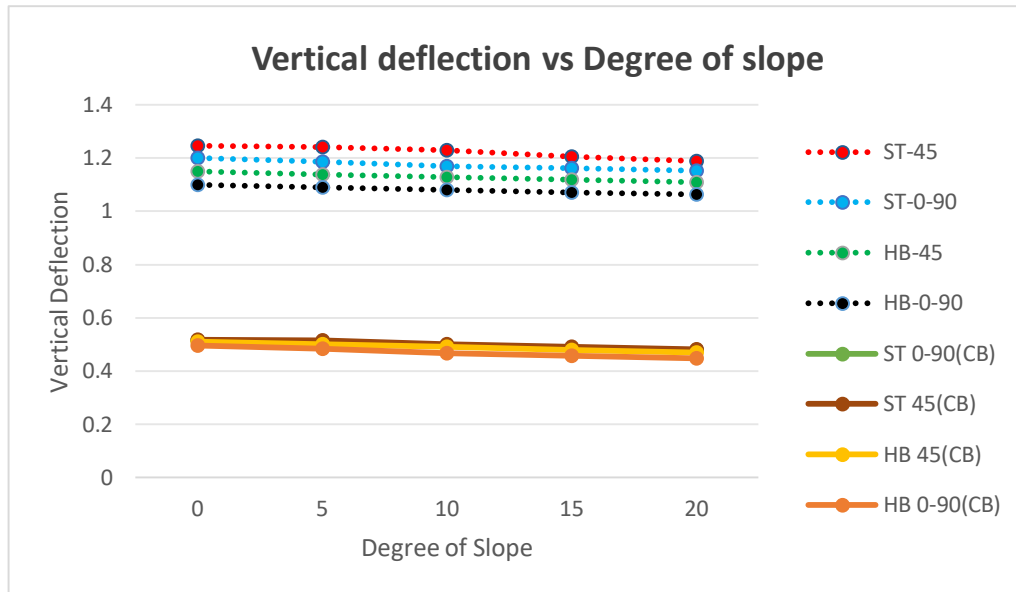


Figure 33: Combined graph of Vertical deflection vs degree of slope

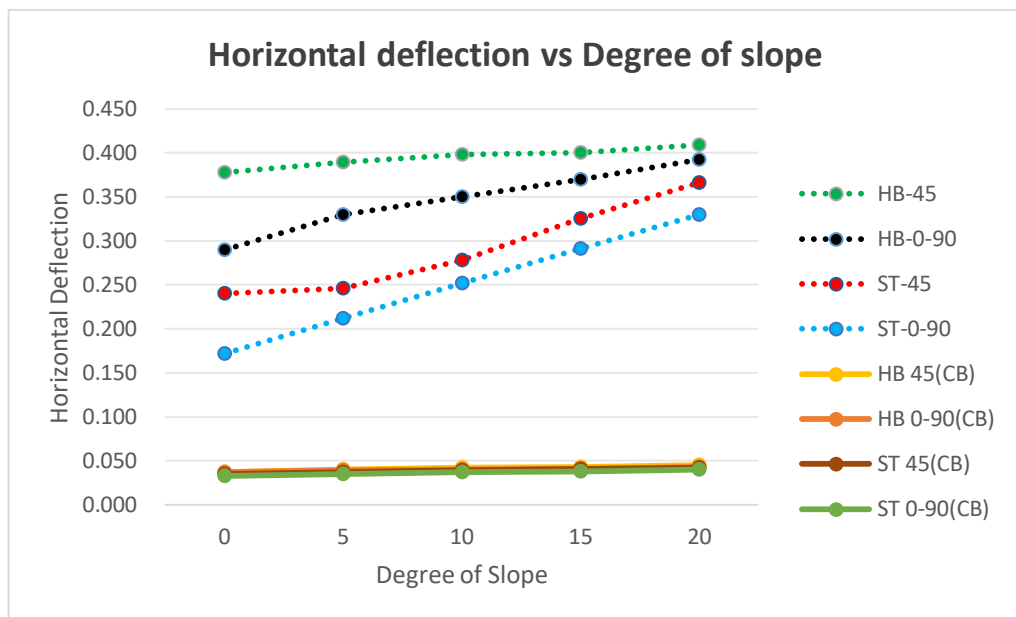


Figure 34: Combined graph of Horizontal deflection vs degree of slope

When observing the combined graph, it is clearly visible how both vertical and horizontal deflections vary with increasing slope angle, and how the implementation of cross beams has affected the block surface. Vertical deflections have been reduced by more than half, while horizontal deflections have decreased significantly by approximately ten times.

Another significant observation was that, due to the horizontal load component, horizontal deflection increased. However, the amount of this increase was significantly lower in block surfaces with cross beams compared to those without.

Therefore, it is evident that the implementation of cross beams on block surfaces has a substantial impact in reducing horizontal deflection, and when cross beams are present, the slope of the block surface has minimal effect on deflection.

5.3. Optimum spacing of cross beams

It was observed that cross beams play a significant role in the stability of road sections with slopes. The spacing between cross beams often varies due to common practices and site conditions. Therefore, it is necessary to analyze the optimum spacing of cross beams and FEM model was developed for sectional lengths of 5 m, 10 m, 15 m, and 20 m to study the effect of cross beam spacing. The same parameters were used as in the previous model, with the degree of slope varying from 0° to 20°, and a 60 kN load applied.

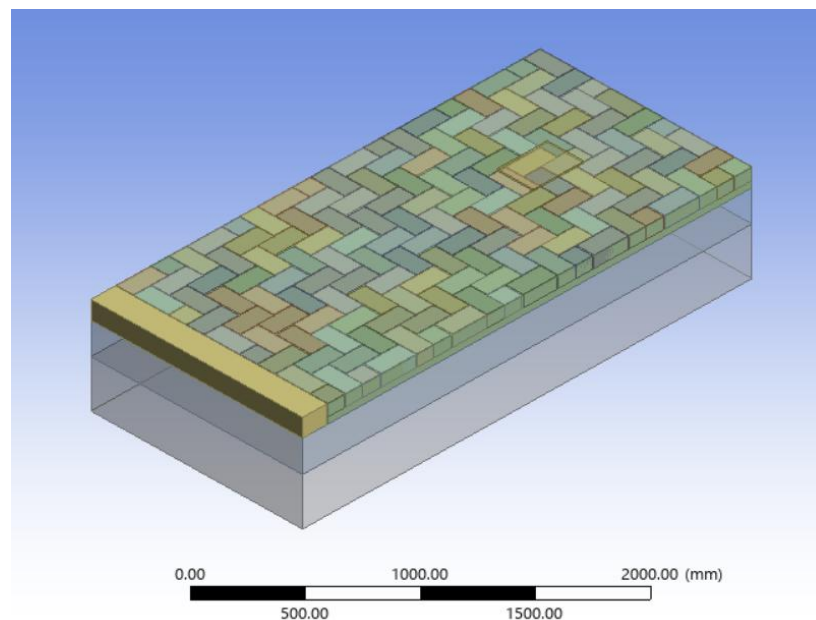


Figure 35: 4m road section developed with ANSYS Workbench

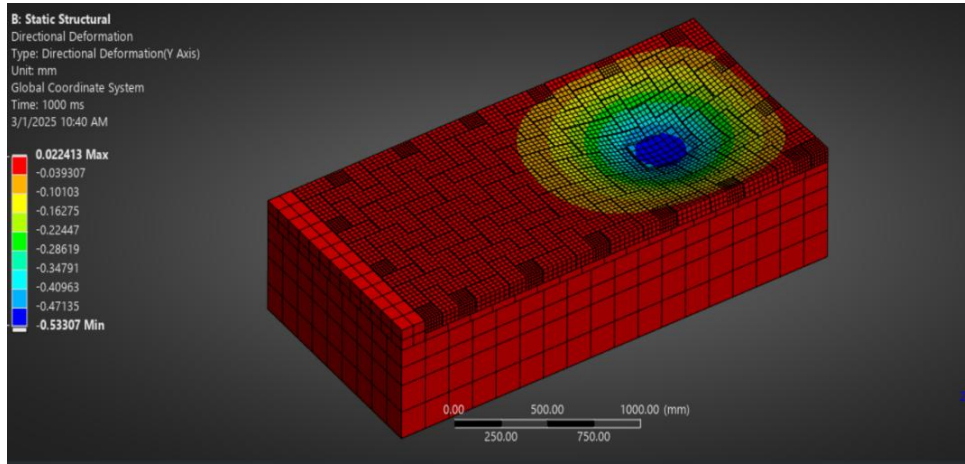
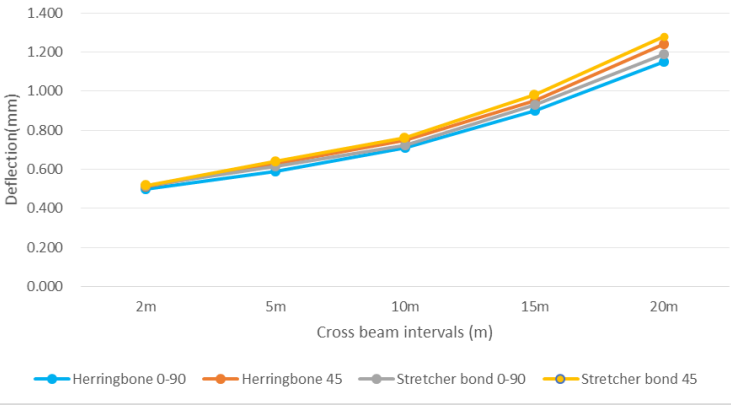
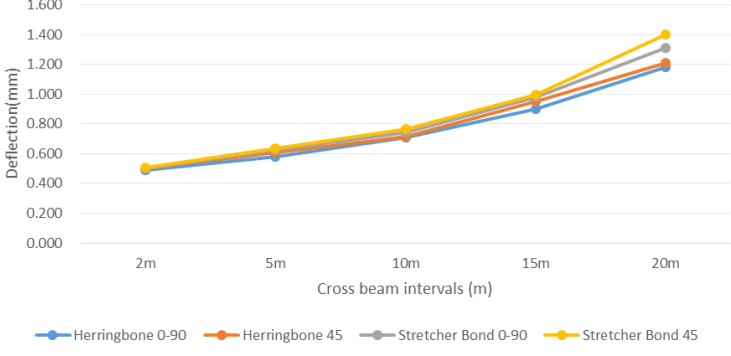
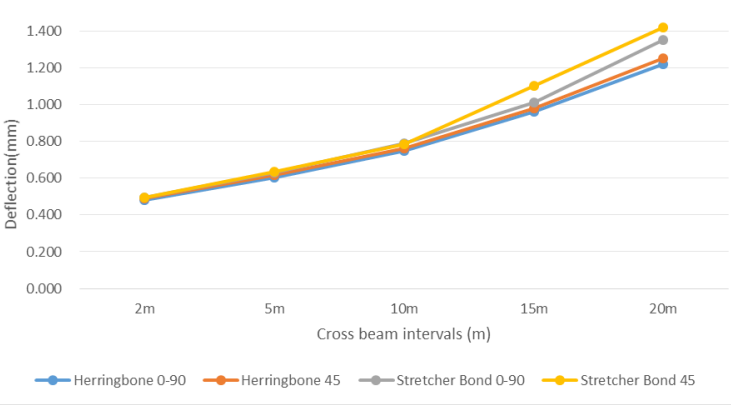


Figure 36: Analysis of 4m road section

Considering degree of slopes from 0^0 to 20^0 , analysis results were obtained for vertical and horizontal deflections for road sections with cross beams(cross beam intervals) starting from 2m to 20m, and graphed as follows.

- **Vertical deflection**

Degree of Slope	Direction of deflection	Graphs																														
0^0	Vertical	<table border="1"> <caption>Approximate data from 'Cross beam intervals vs Vertical deflection' graph</caption> <thead> <tr> <th>Cross beam interval (m)</th> <th>Herringbone 0-90 (mm)</th> <th>Herringbone 45 (mm)</th> <th>Stretcher Bond 0-90 (mm)</th> <th>Stretcher Bond 45 (mm)</th> </tr> </thead> <tbody> <tr> <td>2</td> <td>0.50</td> <td>0.52</td> <td>0.51</td> <td>0.53</td> </tr> <tr> <td>5</td> <td>0.60</td> <td>0.62</td> <td>0.61</td> <td>0.63</td> </tr> <tr> <td>10</td> <td>0.70</td> <td>0.72</td> <td>0.71</td> <td>0.73</td> </tr> <tr> <td>15</td> <td>0.80</td> <td>0.82</td> <td>0.81</td> <td>0.83</td> </tr> <tr> <td>20</td> <td>0.90</td> <td>0.92</td> <td>0.91</td> <td>0.93</td> </tr> </tbody> </table>	Cross beam interval (m)	Herringbone 0-90 (mm)	Herringbone 45 (mm)	Stretcher Bond 0-90 (mm)	Stretcher Bond 45 (mm)	2	0.50	0.52	0.51	0.53	5	0.60	0.62	0.61	0.63	10	0.70	0.72	0.71	0.73	15	0.80	0.82	0.81	0.83	20	0.90	0.92	0.91	0.93
Cross beam interval (m)	Herringbone 0-90 (mm)	Herringbone 45 (mm)	Stretcher Bond 0-90 (mm)	Stretcher Bond 45 (mm)																												
2	0.50	0.52	0.51	0.53																												
5	0.60	0.62	0.61	0.63																												
10	0.70	0.72	0.71	0.73																												
15	0.80	0.82	0.81	0.83																												
20	0.90	0.92	0.91	0.93																												

5 ⁰	Vertical	<p style="text-align: center;">Cross beam intervals vs Vertical deflection</p>  <table border="1" data-bbox="635 257 1369 660"> <thead> <tr> <th>Cross beam intervals (m)</th> <th>Herringbone 0-90 (mm)</th> <th>Herringbone 45 (mm)</th> <th>Stretcher bond 0-90 (mm)</th> <th>Stretcher bond 45 (mm)</th> </tr> </thead> <tbody> <tr> <td>2m</td> <td>0.50</td> <td>0.50</td> <td>0.50</td> <td>0.50</td> </tr> <tr> <td>5m</td> <td>0.60</td> <td>0.60</td> <td>0.60</td> <td>0.65</td> </tr> <tr> <td>10m</td> <td>0.70</td> <td>0.70</td> <td>0.70</td> <td>0.75</td> </tr> <tr> <td>15m</td> <td>0.90</td> <td>0.90</td> <td>0.90</td> <td>0.95</td> </tr> <tr> <td>20m</td> <td>1.15</td> <td>1.15</td> <td>1.15</td> <td>1.28</td> </tr> </tbody> </table>	Cross beam intervals (m)	Herringbone 0-90 (mm)	Herringbone 45 (mm)	Stretcher bond 0-90 (mm)	Stretcher bond 45 (mm)	2m	0.50	0.50	0.50	0.50	5m	0.60	0.60	0.60	0.65	10m	0.70	0.70	0.70	0.75	15m	0.90	0.90	0.90	0.95	20m	1.15	1.15	1.15	1.28
Cross beam intervals (m)	Herringbone 0-90 (mm)	Herringbone 45 (mm)	Stretcher bond 0-90 (mm)	Stretcher bond 45 (mm)																												
2m	0.50	0.50	0.50	0.50																												
5m	0.60	0.60	0.60	0.65																												
10m	0.70	0.70	0.70	0.75																												
15m	0.90	0.90	0.90	0.95																												
20m	1.15	1.15	1.15	1.28																												
10 ⁰	Vertical	<p style="text-align: center;">Cross beam intervals vs Vertical deflection</p>  <table border="1" data-bbox="635 754 1369 1108"> <thead> <tr> <th>Cross beam intervals (m)</th> <th>Herringbone 0-90 (mm)</th> <th>Herringbone 45 (mm)</th> <th>Stretcher Bond 0-90 (mm)</th> <th>Stretcher Bond 45 (mm)</th> </tr> </thead> <tbody> <tr> <td>2m</td> <td>0.50</td> <td>0.50</td> <td>0.50</td> <td>0.50</td> </tr> <tr> <td>5m</td> <td>0.60</td> <td>0.60</td> <td>0.60</td> <td>0.65</td> </tr> <tr> <td>10m</td> <td>0.70</td> <td>0.70</td> <td>0.70</td> <td>0.75</td> </tr> <tr> <td>15m</td> <td>0.90</td> <td>0.90</td> <td>0.90</td> <td>0.95</td> </tr> <tr> <td>20m</td> <td>1.15</td> <td>1.15</td> <td>1.15</td> <td>1.40</td> </tr> </tbody> </table>	Cross beam intervals (m)	Herringbone 0-90 (mm)	Herringbone 45 (mm)	Stretcher Bond 0-90 (mm)	Stretcher Bond 45 (mm)	2m	0.50	0.50	0.50	0.50	5m	0.60	0.60	0.60	0.65	10m	0.70	0.70	0.70	0.75	15m	0.90	0.90	0.90	0.95	20m	1.15	1.15	1.15	1.40
Cross beam intervals (m)	Herringbone 0-90 (mm)	Herringbone 45 (mm)	Stretcher Bond 0-90 (mm)	Stretcher Bond 45 (mm)																												
2m	0.50	0.50	0.50	0.50																												
5m	0.60	0.60	0.60	0.65																												
10m	0.70	0.70	0.70	0.75																												
15m	0.90	0.90	0.90	0.95																												
20m	1.15	1.15	1.15	1.40																												
15 ⁰	Vertical	<p style="text-align: center;">Cross beam intervals vs Vertical deflection</p>  <table border="1" data-bbox="635 1198 1369 1601"> <thead> <tr> <th>Cross beam intervals (m)</th> <th>Herringbone 0-90 (mm)</th> <th>Herringbone 45 (mm)</th> <th>Stretcher Bond 0-90 (mm)</th> <th>Stretcher Bond 45 (mm)</th> </tr> </thead> <tbody> <tr> <td>2m</td> <td>0.50</td> <td>0.50</td> <td>0.50</td> <td>0.50</td> </tr> <tr> <td>5m</td> <td>0.60</td> <td>0.60</td> <td>0.60</td> <td>0.65</td> </tr> <tr> <td>10m</td> <td>0.70</td> <td>0.70</td> <td>0.70</td> <td>0.75</td> </tr> <tr> <td>15m</td> <td>0.90</td> <td>0.90</td> <td>0.90</td> <td>0.95</td> </tr> <tr> <td>20m</td> <td>1.15</td> <td>1.15</td> <td>1.15</td> <td>1.40</td> </tr> </tbody> </table>	Cross beam intervals (m)	Herringbone 0-90 (mm)	Herringbone 45 (mm)	Stretcher Bond 0-90 (mm)	Stretcher Bond 45 (mm)	2m	0.50	0.50	0.50	0.50	5m	0.60	0.60	0.60	0.65	10m	0.70	0.70	0.70	0.75	15m	0.90	0.90	0.90	0.95	20m	1.15	1.15	1.15	1.40
Cross beam intervals (m)	Herringbone 0-90 (mm)	Herringbone 45 (mm)	Stretcher Bond 0-90 (mm)	Stretcher Bond 45 (mm)																												
2m	0.50	0.50	0.50	0.50																												
5m	0.60	0.60	0.60	0.65																												
10m	0.70	0.70	0.70	0.75																												
15m	0.90	0.90	0.90	0.95																												
20m	1.15	1.15	1.15	1.40																												

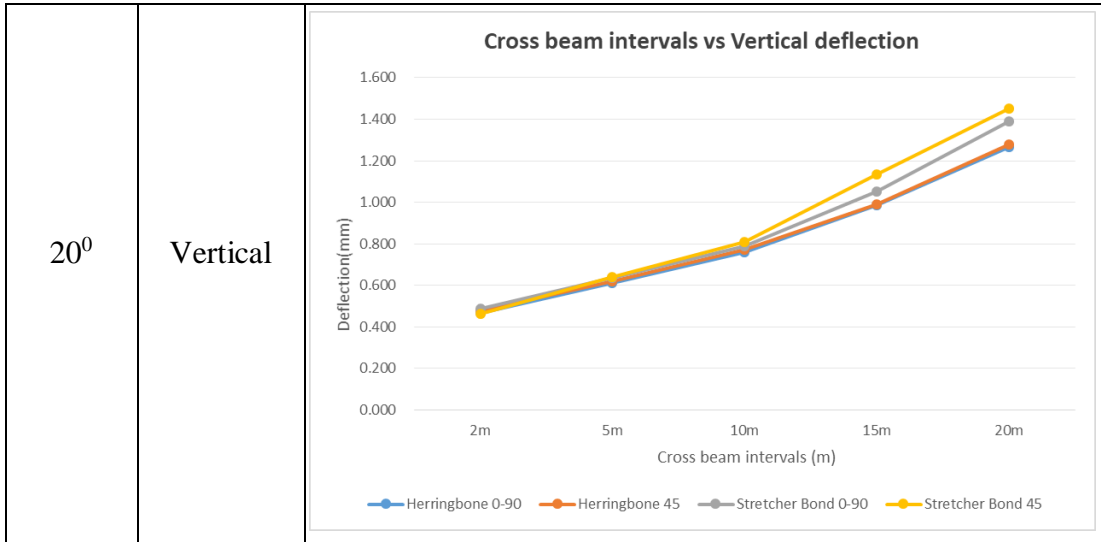


Table 11: Vertical deflection graphs from 0° to 20°

- Horizontal deflection**

Degree of Slope	Direction of deflection	Graphs																														
0°	Horizontal	<table border="1"> <caption>Data for Cross beam intervals vs Horizontal deflection (0°)</caption> <thead> <tr> <th>Cross beam intervals (m)</th> <th>Herringbone 0-90 (mm)</th> <th>Herringbone 45 (mm)</th> <th>Stretcher Bond 0-90 (mm)</th> <th>Stretcher Bond 45 (mm)</th> </tr> </thead> <tbody> <tr> <td>2m</td> <td>0.035</td> <td>0.035</td> <td>0.035</td> <td>0.035</td> </tr> <tr> <td>5m</td> <td>0.045</td> <td>0.045</td> <td>0.045</td> <td>0.045</td> </tr> <tr> <td>10m</td> <td>0.055</td> <td>0.055</td> <td>0.055</td> <td>0.055</td> </tr> <tr> <td>15m</td> <td>0.065</td> <td>0.065</td> <td>0.065</td> <td>0.065</td> </tr> <tr> <td>20m</td> <td>0.085</td> <td>0.085</td> <td>0.085</td> <td>0.090</td> </tr> </tbody> </table>	Cross beam intervals (m)	Herringbone 0-90 (mm)	Herringbone 45 (mm)	Stretcher Bond 0-90 (mm)	Stretcher Bond 45 (mm)	2m	0.035	0.035	0.035	0.035	5m	0.045	0.045	0.045	0.045	10m	0.055	0.055	0.055	0.055	15m	0.065	0.065	0.065	0.065	20m	0.085	0.085	0.085	0.090
Cross beam intervals (m)	Herringbone 0-90 (mm)	Herringbone 45 (mm)	Stretcher Bond 0-90 (mm)	Stretcher Bond 45 (mm)																												
2m	0.035	0.035	0.035	0.035																												
5m	0.045	0.045	0.045	0.045																												
10m	0.055	0.055	0.055	0.055																												
15m	0.065	0.065	0.065	0.065																												
20m	0.085	0.085	0.085	0.090																												
5°	Horizontal	<table border="1"> <caption>Data for Cross beam intervals vs Horizontal deflection (5°)</caption> <thead> <tr> <th>Cross beam intervals (m)</th> <th>Herringbone 0-90 (mm)</th> <th>Herringbone 45 (mm)</th> <th>Stretcher Bond 0-90 (mm)</th> <th>Stretcher Bond 45 (mm)</th> </tr> </thead> <tbody> <tr> <td>2m</td> <td>0.040</td> <td>0.040</td> <td>0.040</td> <td>0.040</td> </tr> <tr> <td>5m</td> <td>0.055</td> <td>0.055</td> <td>0.055</td> <td>0.055</td> </tr> <tr> <td>10m</td> <td>0.085</td> <td>0.085</td> <td>0.085</td> <td>0.085</td> </tr> <tr> <td>15m</td> <td>0.120</td> <td>0.120</td> <td>0.120</td> <td>0.120</td> </tr> <tr> <td>20m</td> <td>0.210</td> <td>0.210</td> <td>0.210</td> <td>0.250</td> </tr> </tbody> </table>	Cross beam intervals (m)	Herringbone 0-90 (mm)	Herringbone 45 (mm)	Stretcher Bond 0-90 (mm)	Stretcher Bond 45 (mm)	2m	0.040	0.040	0.040	0.040	5m	0.055	0.055	0.055	0.055	10m	0.085	0.085	0.085	0.085	15m	0.120	0.120	0.120	0.120	20m	0.210	0.210	0.210	0.250
Cross beam intervals (m)	Herringbone 0-90 (mm)	Herringbone 45 (mm)	Stretcher Bond 0-90 (mm)	Stretcher Bond 45 (mm)																												
2m	0.040	0.040	0.040	0.040																												
5m	0.055	0.055	0.055	0.055																												
10m	0.085	0.085	0.085	0.085																												
15m	0.120	0.120	0.120	0.120																												
20m	0.210	0.210	0.210	0.250																												

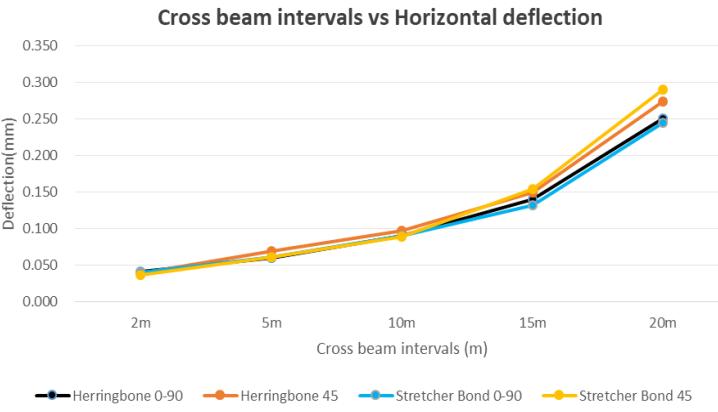
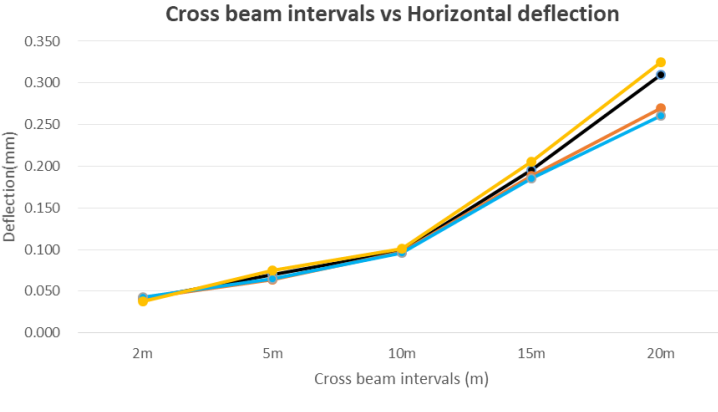
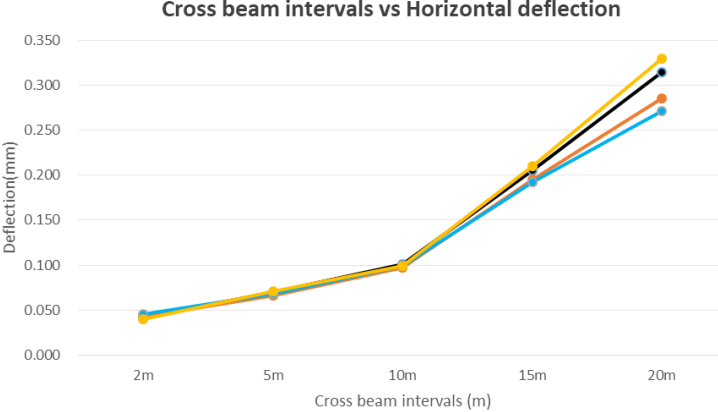
10 ⁰	Horizontal	 <p>Cross beam intervals vs Horizontal deflection</p> <table border="1"> <thead> <tr> <th>Cross beam intervals (m)</th> <th>Herringbone 0-90 (mm)</th> <th>Herringbone 45 (mm)</th> <th>Stretcher Bond 0-90 (mm)</th> <th>Stretcher Bond 45 (mm)</th> </tr> </thead> <tbody> <tr> <td>2m</td> <td>0.04</td> <td>0.04</td> <td>0.04</td> <td>0.04</td> </tr> <tr> <td>5m</td> <td>0.06</td> <td>0.06</td> <td>0.06</td> <td>0.06</td> </tr> <tr> <td>10m</td> <td>0.09</td> <td>0.09</td> <td>0.09</td> <td>0.09</td> </tr> <tr> <td>15m</td> <td>0.13</td> <td>0.13</td> <td>0.13</td> <td>0.15</td> </tr> <tr> <td>20m</td> <td>0.24</td> <td>0.26</td> <td>0.24</td> <td>0.29</td> </tr> </tbody> </table>	Cross beam intervals (m)	Herringbone 0-90 (mm)	Herringbone 45 (mm)	Stretcher Bond 0-90 (mm)	Stretcher Bond 45 (mm)	2m	0.04	0.04	0.04	0.04	5m	0.06	0.06	0.06	0.06	10m	0.09	0.09	0.09	0.09	15m	0.13	0.13	0.13	0.15	20m	0.24	0.26	0.24	0.29
Cross beam intervals (m)	Herringbone 0-90 (mm)	Herringbone 45 (mm)	Stretcher Bond 0-90 (mm)	Stretcher Bond 45 (mm)																												
2m	0.04	0.04	0.04	0.04																												
5m	0.06	0.06	0.06	0.06																												
10m	0.09	0.09	0.09	0.09																												
15m	0.13	0.13	0.13	0.15																												
20m	0.24	0.26	0.24	0.29																												
15 ⁰	Horizontal	 <p>Cross beam intervals vs Horizontal deflection</p> <table border="1"> <thead> <tr> <th>Cross beam intervals (m)</th> <th>Herringbone 0-90 (mm)</th> <th>Herringbone 45 (mm)</th> <th>Stretcher Bond 0-90 (mm)</th> <th>Stretcher Bond 45 (mm)</th> </tr> </thead> <tbody> <tr> <td>2m</td> <td>0.04</td> <td>0.04</td> <td>0.04</td> <td>0.04</td> </tr> <tr> <td>5m</td> <td>0.06</td> <td>0.06</td> <td>0.06</td> <td>0.06</td> </tr> <tr> <td>10m</td> <td>0.09</td> <td>0.09</td> <td>0.09</td> <td>0.09</td> </tr> <tr> <td>15m</td> <td>0.19</td> <td>0.19</td> <td>0.18</td> <td>0.20</td> </tr> <tr> <td>20m</td> <td>0.31</td> <td>0.27</td> <td>0.26</td> <td>0.32</td> </tr> </tbody> </table>	Cross beam intervals (m)	Herringbone 0-90 (mm)	Herringbone 45 (mm)	Stretcher Bond 0-90 (mm)	Stretcher Bond 45 (mm)	2m	0.04	0.04	0.04	0.04	5m	0.06	0.06	0.06	0.06	10m	0.09	0.09	0.09	0.09	15m	0.19	0.19	0.18	0.20	20m	0.31	0.27	0.26	0.32
Cross beam intervals (m)	Herringbone 0-90 (mm)	Herringbone 45 (mm)	Stretcher Bond 0-90 (mm)	Stretcher Bond 45 (mm)																												
2m	0.04	0.04	0.04	0.04																												
5m	0.06	0.06	0.06	0.06																												
10m	0.09	0.09	0.09	0.09																												
15m	0.19	0.19	0.18	0.20																												
20m	0.31	0.27	0.26	0.32																												
20 ⁰	Horizontal	 <p>Cross beam intervals vs Horizontal deflection</p> <table border="1"> <thead> <tr> <th>Cross beam intervals (m)</th> <th>Herringbone 0-90 (mm)</th> <th>Herringbone 45 (mm)</th> <th>Stretcher Bond 0-90 (mm)</th> <th>Stretcher Bond 45 (mm)</th> </tr> </thead> <tbody> <tr> <td>2m</td> <td>0.04</td> <td>0.04</td> <td>0.04</td> <td>0.04</td> </tr> <tr> <td>5m</td> <td>0.06</td> <td>0.06</td> <td>0.06</td> <td>0.06</td> </tr> <tr> <td>10m</td> <td>0.09</td> <td>0.09</td> <td>0.09</td> <td>0.09</td> </tr> <tr> <td>15m</td> <td>0.20</td> <td>0.20</td> <td>0.19</td> <td>0.21</td> </tr> <tr> <td>20m</td> <td>0.31</td> <td>0.28</td> <td>0.27</td> <td>0.33</td> </tr> </tbody> </table>	Cross beam intervals (m)	Herringbone 0-90 (mm)	Herringbone 45 (mm)	Stretcher Bond 0-90 (mm)	Stretcher Bond 45 (mm)	2m	0.04	0.04	0.04	0.04	5m	0.06	0.06	0.06	0.06	10m	0.09	0.09	0.09	0.09	15m	0.20	0.20	0.19	0.21	20m	0.31	0.28	0.27	0.33
Cross beam intervals (m)	Herringbone 0-90 (mm)	Herringbone 45 (mm)	Stretcher Bond 0-90 (mm)	Stretcher Bond 45 (mm)																												
2m	0.04	0.04	0.04	0.04																												
5m	0.06	0.06	0.06	0.06																												
10m	0.09	0.09	0.09	0.09																												
15m	0.20	0.20	0.19	0.21																												
20m	0.31	0.28	0.27	0.33																												

Table 12: Horizontal deflection graphs from 0⁰ to 20⁰

Observing the above graphs indicates that as the spacing between cross beams (cross beam intervals) increases, both horizontal and vertical deflections increase uniformly. However, when the degree of slope increases, this uniformity breaks at a certain point, and the rate of deflection increase becomes significantly higher. This suggests a correlation between the degree of slope and cross beam spacing.

Based on these observations, the best-performing block paving pattern which is herringbone was selected, and two graphs were plotted showing vertical and horizontal deflection versus cross beam intervals for different slope angles.

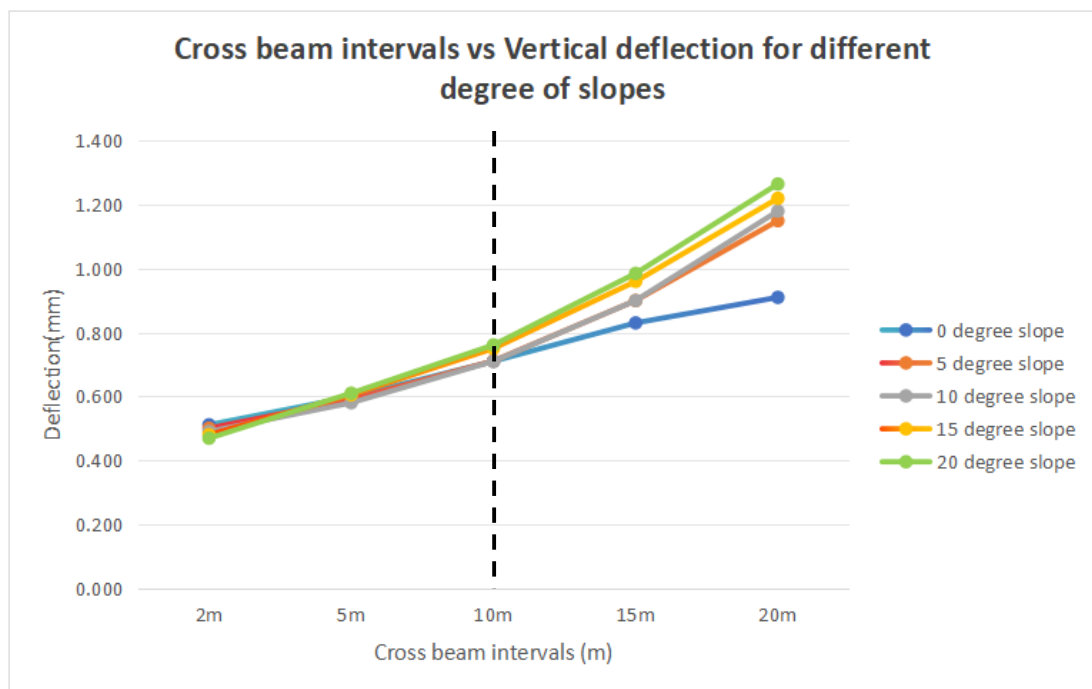


Figure 37: Cross beam intervals vs vertical deflection for different degree of slopes

It was observed that as the road section length (spacing between cross beams) increases, sections with a 0° slope show a uniform increase in deflection. However, when the slope angle increases, this uniformity breaks at a section length of 10 m, beyond which vertical deflection increases drastically.

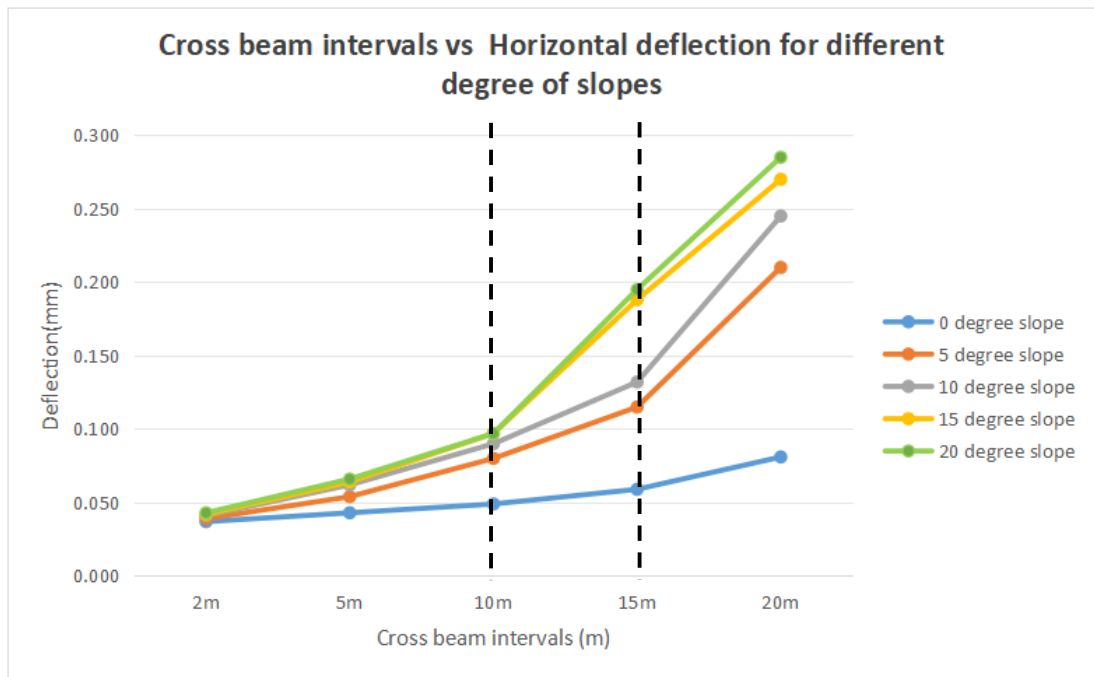


Figure 38: Cross beam intervals vs vertical deflection for different degree of slopes

A different scenario was observed in the road section length vs. horizontal deflection graph. The uniform increase in horizontal deflection breaks at a road length of 15 m for the 5° and 10° slope graphs, whereas for the 15° and 20° slope graphs, this uniformity breaks at 10 m.

This indicates that for road sections with a slope angle up to 10°, cross beam spacing can be effectively maintained at 15 m intervals. However, for slopes greater than 10°, a 10 m spacing between cross beams is more appropriate. Nevertheless, when considering both vertical and horizontal deflection graphs, it is recommended to adopt a 10 m cross beam spacing for all sloped road sections to ensure overall structural stability.

6.0 CONCLUSION

The average vertical deflection measured from the field data of the trial section ranged from -3 mm to -4 mm. When compared with the FEM model results, these deflections were significantly higher. This difference is likely due to the uncontrolled nature of the field site, where construction quality and external variables could not be regulated unlike in a laboratory-scale environment. Therefore, field measurements should be interpreted as indicative rather than directly comparable with the FEM outputs.

Upon validating the FEM model, simulations were conducted under varying block laying conditions, including different block patterns, laying angles, and slope gradients from 0° to 20°. Results showed that in the absence of cross beams, both vertical and horizontal deflections increased with slope, and were strongly affected by block pattern and laying angle. Among the tested configurations, the herringbone pattern performed best. However, when cross beams were introduced, deflections decreased significantly, and the impact of slope, pattern, and angle became minimal.

These simulations were based on a 2-meter road segment and later extended to investigate the effect of cross beam spacing up to 20 meters. The analysis suggests that for road slopes up to 10°, cross beams spaced at 10 to 15 meters are sufficient, while slopes between 10° and 20° require a maximum 10-meter spacing. From a structural performance perspective, 10-meter cross beam spacing provides the best balance between constructability and deflection control across sloped terrains.

It is also important to acknowledge several limitations. The FEM model used cobble block geometry instead of the Uni-style blocks commonly used in Sri Lanka, due to software constraints. The analysis assumed only a single axle static load and did not include dynamic effects such as braking forces. Furthermore, the influence of varying joint width spacing, sand filling, and higher traffic volumes were not considered. These factors could affect deflection behavior and should be explored in future research.

Based on the current findings and within these limitations, it is concluded that concrete block paving can be used effectively on rural road slopes up to 15°, provided that cross beams are installed at 10-meter intervals. Slopes exceeding 15° may not be practical for rural road construction due to vehicle navigation issues and increasing instability under higher loads. Future work should investigate higher slopes, variable traffic loads,

braking effects, and different block geometries to extend the applicability of these findings.

7.0 LIMITATIONS AND RECOMMENDATIONS

Uni-style blocks are the most commonly used interlocking block type for rural road paving in Sri Lanka. However, due to geometric limitations, this block type cannot be directly modeled within ANSYS Workbench. Instead, the geometry must first be developed in SolidWorks and then imported into ANSYS Workbench. Given this constraint, cobble-style block geometry was adopted in the finite element (FEM) model for this study.

This research primarily focused on determining the maximum permissible slope for block paving, specifically in the context of Sri Lankan rural roads. These roads often serve as vital connections between small communities and main roads, typically experiencing low traffic volumes. However, in certain hill country areas, rural roads can have slopes exceeding 20° , and in some cases, these roads function as the main access route for villages, leading to increased traffic demands.

In this study, a single axle load was applied in the FEM analysis. It is recommended that future research incorporate a range of axle loads to reflect varying traffic demands. Such investigations could also analyze the relationship between axle loads and optimal cross beam spacing, which is a key factor in resisting block creep on sloped pavements.

As noted, the analysis in this study was limited to a maximum slope of 20° due to time constraints. However, practical observations indicate that steeper slopes exist in upcountry regions. Therefore, future research should extend the analysis beyond 20° , particularly to assess cross beam spacing requirements for slopes greater than this value. This would provide more applicable and comprehensive design guidance for rural roads in hilly areas.

The FEM model used a fixed joint width spacing of 5 mm with sand filling. It is advisable for future studies to investigate the effects of varying joint widths and analyze whether there is a correlation between joint width spacing, slope angle, and required cross beam spacing. This could provide critical insight into joint behavior and its influence on pavement stability under inclined conditions.

Moreover, only static load and frictional force were considered in the current FEM analysis. The influence of braking forces especially relevant on sloped roads was not

accounted for. Future models should incorporate braking effects to enhance the reliability of the simulation and better reflect real-world driving conditions.

8.0 REFERENCES

CONCRETE BLOCK PAVING A walk-over in cost, looks and durability for Concrete Block Paving Technical note for steep slopes. (n.d.).

Gunatilake, D., & Mampearachchi, W. K. (2019). Finite element modelling approach to determine optimum dimensions for interlocking concrete blocks used for road paving. *Road Materials and Pavement Design*, 20(2), 280–296. <https://doi.org/10.1080/14680629.2017.1385512>

Mampearachchi, W. K., & Gunarathna, W. P. H. (2010). Finite-Element Model Approach to Determine Support Conditions and Effective Layout for Concrete Block Paving. *Journal of Materials in Civil Engineering*, 22(11), 1139–1147. [https://doi.org/10.1061/\(ASCE\)MT.1943-5533.0000118](https://doi.org/10.1061/(ASCE)MT.1943-5533.0000118)

Mampearachchi, W. K., & Senadeera, A. (2014). Determination of the Most Effective Cement Concrete Block Laying Pattern and Shape for Road Pavement Based on Field Performance. *Journal of Materials in Civil Engineering*, 26(2), 226–232. [https://doi.org/10.1061/\(ASCE\)MT.1943-5533.0000801](https://doi.org/10.1061/(ASCE)MT.1943-5533.0000801)

Miura, Y., Takaura, M., Tsuda, T., & Co, C. K. H. (n.d.). *STRUCTURAL DESIGN OF CONCRETE BLOCK PAVEMENTS BY CBR METHOD AND ITS EVALUATION*.

Mudiyono, R. (2015). *The Effect of Paver Joint Width on the Construction of Concrete Block Pavement on Sloping Road Section*.

Murat Algin, H. (2007). Interlock Mechanism of Concrete Block Pavements. *Journal of Transportation Engineering*, 133(5), 318–326. [https://doi.org/10.1061/\(ASCE\)0733-947X\(2007\)133:5\(318\)](https://doi.org/10.1061/(ASCE)0733-947X(2007)133:5(318))

Panda, B. C., & Ghosh, A. K. (2002a). Structural Behavior of Cast In Situ Concrete Block Pavement. *Journal of Transportation Engineering*, 131(9), 662–668. [https://doi.org/10.1061/\(ASCE\)0733-947X\(2005\)131:9\(662\)](https://doi.org/10.1061/(ASCE)0733-947X(2005)131:9(662))

Shackel, B. (n.d.). *The Challenges of Concrete Block Paving as a Mature Technology*.

9.0 APPENDIX

Appendix A-1

Levels of the wheel path after construction before allowing traffic

Chainage	Wheel path	
	LHS	RHS
0+000	100.100	100.105
0+002	100.360	100.366
0+004	100.621	100.629
0+006	100.881	100.894
0+008	101.152	101.161
0+010	101.414	101.426
0+012	101.679	101.690
0+014	101.948	101.953
0+016	102.211	102.217
0+018	102.476	102.483
0+020	102.742	102.748
0+022	103.003	103.013
0+024	103.261	103.274
0+026	103.522	103.536
0+028	103.781	103.800
0+030	104.041	104.065
0+032	104.302	104.331
0+034	104.567	104.594
0+036	104.829	104.848
0+038	105.091	105.104
0+040	105.354	105.369
0+042	105.622	105.625
0+044	105.884	105.885
0+046	106.149	106.146
0+048	106.413	106.410
0+050	106.679	106.671
0+052	106.940	106.935
0+054	107.205	107.194

0+056	107.467	107.459
0+058	107.730	107.725
0+060	107.995	107.990
0+062	108.257	108.256
0+064	108.520	108.516
0+066	108.782	108.776
0+068	109.045	109.042
0+070	109.312	109.307
0+072	109.580	109.571
0+074	109.845	109.837
0+076	110.108	110.103
0+078	110.370	110.370
0+080	110.634	110.631
0+082	110.899	110.896
0+084	111.165	111.160
0+086	111.430	111.428
0+088	111.695	111.696
0+090	111.964	111.963

Appendix A-2

Levels of wheel path after 6 months allowing traffic

Chainage	Wheel path	
	LHS	RHS
0+000	100.102	100.108
0+002	100.361	100.368
0+004	100.623	100.632
0+006	100.882	100.897
0+008	101.155	101.163
0+010	101.417	101.430
0+012	101.681	101.694
0+014	101.952	101.956
0+016	102.212	102.220
0+018	102.480	102.487

0+020	102.745	102.750
0+022	103.008	103.017
0+024	103.264	103.277
0+026	103.524	103.540
0+028	103.784	103.804
0+030	104.046	104.070
0+032	104.304	104.334
0+034	104.570	104.597
0+036	104.831	104.849
0+038	105.094	105.108
0+040	105.358	105.373
0+042	105.625	105.627
0+044	105.889	105.889
0+046	106.152	106.149
0+048	106.415	106.414
0+050	106.682	106.674
0+052	106.942	106.939
0+054	107.208	107.198
0+056	107.472	107.464
0+058	107.733	107.729
0+060	107.997	107.994
0+062	108.261	108.259
0+064	108.521	108.519
0+066	108.786	108.780
0+068	109.048	109.044
0+070	109.317	109.311
0+072	109.583	109.574
0+074	109.847	109.841
0+076	110.110	110.107
0+078	110.373	110.373
0+080	110.636	110.635
0+082	110.902	110.900
0+084	111.170	111.165
0+086	111.433	111.432
0+088	111.697	111.700
0+090	111.968	111.966